

classes of vaccines, such as live attenuated vaccines and DNA vaccines. Emerging evidence also supports the concept that nucleic acids and their metabolites are important endogenous mediators of the adjuvant effects of aluminium salt-based adjuvants (commonly referred to as alum), an important class of vaccine adjuvants. This knowledge could provide useful hints for the design and optimization of future vaccines.

Deconstructing live vaccines. Some live attenuated vaccines are among the most efficient vaccines ever developed. Although live attenuated vaccines cannot be generated against all types of pathogen, deconstructing the responses they induce may offer valuable clues for the design of new vaccines that mimic their mechanisms of action. Few studies have addressed this so far, but the data are starting to point towards a central role of nucleic acid-sensing PRRs in the response to live attenuated vaccines.

The yellow fever vaccine YF-17D is one of the most efficient antiviral vaccines ever developed, and it is able to induce protective immunity that lasts for decades. Evidence in mice indicates that YF-17D activates DCs through the concomitant stimulation of several TLRs (namely, TLR2, TLR7, TLR8 and TLR9), which results in the induction of CD8⁺ T cell responses and a mixed T_{H1}- and T_{H2}-type immune response⁵⁰. Although TLR2 signalling, which depends on MYD88, appears to downregulate the T_{H1} and CD8⁺ T cell responses elicited by the vaccine, MYD88-dependent signalling is required for these responses. Without ruling out a potential contribution of IL-1 and related cytokines or other MYD88-dependent PRRs, these results suggest an important role for nucleic acid-sensing TLRs in the induction of adaptive T_{H1}-type responses to YF-17D. In support of this assumption, DCs from mice deficient for either TLR7 or TLR9 secrete less IL-12 than wild-type DCs following infection with YF-17D⁵⁰. In vaccinated humans, gene expression profiling indicates that YF-17D activates a prominent type I IFN response (which is probably controlled by IRF7) at the time the primary adaptive immune response is established^{51,52}. Furthermore, YF-17D upregulates the expression of TLR7 (REF 51) and activates RIG-I and MDA5 (REF 52), although the contribution of these receptors to adaptive immune responses in this context is currently unknown. Finally, a recent study in humans indicates that YF-17D induces innate immune gene expression profiles that functionally overlap with those elicited by an experimental adjuvant that is based on a modified polyI:C agonist of TLR3 and MDA5 (REF 53).

Vaccinia virus is the attenuated virus that formed the basis of the vaccine that allowed the eradication of smallpox. It is now used as a vector in other vaccines. Vaccinia virus may activate several APC-expressed PRRs, including RIG-I, MDA5, TLR2, TLR6, TLR9 and NLRP3- and AIM2-dependent inflammasomes^{41,54,55}. Studies in knock-out mice have revealed that the activation of innate immune responses and the induction of CD8⁺ T cell population expansion and memory formation in response to vaccinia virus crucially depend on TLR2 (REF 56), but also require type I IFN

production^{56,57}. Moreover, a recent report suggests that, in mice, type I IFN production following vaccinia virus infection may result from TLR8-dependent activation of pDCs, possibly through the recognition of AT-rich DNA⁵⁸. Whether this mechanism also occurs in humans, whose pDCs do not express TLR8, is not yet certain. In addition, cDCs may produce type I IFNs following vaccinia virus infection in a TLR-independent manner, probably through TLR-dependent signalling^{55,56}.

In the case of influenza A virus, a variety of vaccine compositions have been developed, including live attenuated, killed whole-virion and subunit vaccines. The influenza virus ssRNA genome has been shown to activate pDCs through TLR7 (REFS 59,60) and cDCs and stromal cells through RIG-I-dependent sensing^{61,62}. Influenza virus RNA also indirectly triggers inflammasome activation^{35,36,63}. Subunit vaccines, which are devoid of viral RNA, were shown to be ineffective at immunizing naive mice owing to their inability to stimulate pDCs, although they could still boost memory T cell responses⁶⁴. This evidence underscores the importance of viral nucleic acid sensing in influenza vaccination. By contrast, live attenuated and killed vaccines induce robust primary adaptive immune responses through TLR7, a process that requires the production of type I IFNs by pDCs in the case of killed vaccines^{64,65}.

Very few studies so far have investigated the role of nucleic acid-sensing PRRs in live attenuated bacterial vaccines. The immunogenicity of such vaccines — which include the *Mycobacterium bovis* bacillus Calmette-Guérin (BCG) vaccine — is usually attributed to the innate recognition of bacterial cell wall components, mostly by TLR2 and TLR4. However, live bacteria may also activate APCs through nucleic acid-sensing PRRs^{17,22,66,67}. Recent research indicates that nucleic acid sensing could actually be key to the success of live bacterial vaccines.

One possible explanation for the higher efficiency of live attenuated bacterial vaccines over killed vaccines could be that the immune system is able somehow to sense general bacterial viability. This possibility has recently received support from an elegant study that compared the innate and adaptive immune responses induced by live and killed non-replicating non-virulent bacteria⁶⁸. Live bacteria, but not killed bacteria, were shown to induce pronounced expression of type I IFNs and the release of mature IL-1 β from infected macrophages and DCs. The augmented response to live bacteria was shown to depend on the sensing of bacterial mRNA, which is lost following the killing of the bacteria and was therefore termed a viability-associated PAMP ('vita-PAMP'). The cytosolic PRR responsible for vita-PAMP sensing in this context has not been identified, but the induction of type I IFNs by IRF3 and the generation of IL-1 β by the NLRP3 inflammasome were impaired in TRIF-deficient cells. The recognition of this vita-PAMP was proposed to depend on the absence of 3'-polyadenylation in bacterial mRNA. Consistent with the idea that vita-PAMP sensing may boost adaptive immune responses, killed bacteria mixed with bacterial mRNA were shown to induce humoral responses similar to those induced by live bacteria in mice.

Molecular mechanisms of DNA vaccination. DNA vaccines are one example of vector-based vaccines that are currently in development⁶⁹. What is considered a major advantage of DNA vaccines is their ability to induce the local expression of target antigens and to subsequently elicit T_H1 and CD8⁺ T cell responses along with T_H1 -biased antibody production. DNA vaccines are currently used in veterinary medicine, and attempts in humans indicate a good tolerability and safety profile^{69,70}. However, DNA vaccines tend to display low immunogenicity in humans and this has hindered their development, although different approaches have been proposed to address this issue. The reasons for this lower responsiveness of humans compared with other mammals are currently unclear. Possible explanations could involve lower expression levels of certain components of the DNA-sensing machinery, differing expression patterns of nucleic acid-sensing PRRs or issues related to DNA delivery and processing in different cell types^{69,70}. It is likely that a more accurate characterization of the cellular and molecular mechanisms involved in nucleic acid sensing during DNA vaccination would help us to understand these issues and improve the design of such vaccines.

The plasmids used in DNA vaccination may contain CpG motifs, which would provide a built-in adjuvant because these PAMPs activate TLR9. However, TLR9 deficiency does not appear to affect the cellular or humoral immune responses to repeated DNA vaccination in mice^{71,72}, although TLR9 could participate in CD8⁺ T cell induction following the initial immunization⁷³. Instead, T_H1 and CD8⁺ T cell responses, as well as antibody production, in response to DNA vaccination in mice have been shown to crucially depend on the induction of type I IFNs through the STING–TBK1 axis^{72,74}. Although the PRR implicated in DNA detection in this context remains to be identified, this suggests that cytoplasmic receptors for DNA have a more prominent role than intracellular TLRs in mediating the effect of DNA vaccines. Given that STING engagement may also lead to NF- κ B activation⁷⁴, it could be worthwhile investigating the potential contribution of this pathway in DNA vaccination.

DNA vaccine administration may lead to the direct transfection of APCs or to the transfection of other tissue-resident cells, such as muscle cells. In the latter case, antigens may be indirectly acquired by DCs for presentation⁹⁹. Bone marrow transfer experiments in mice support the idea that antibody responses to DNA vaccination require TBK1 activation in haematopoietic cells (presumably DCs)⁷². By contrast, TBK1 activity in non-haematopoietic cells (presumably stromal cells) is essential for CD8⁺ T cell activation. Finally, the activation of antigen-specific CD4⁺ T cells requires TBK1 activity in both the haematopoietic and non-haematopoietic compartments. Altogether, direct presentation, cross-presentation and bystander cytokine production are all likely to be essential for the adaptive immune response to DNA vaccines (FIG 3).

Cross-presentation
A process by which certain antigen-presenting cells may take up and process extracellular antigens and present them on MHC class I molecules to CD8⁺ T cells

Nucleic tricks of an old adjuvant. Alum is the oldest but most widely used of the few vaccine adjuvants that are licensed for human use⁷⁵. Alum mostly potentiates IgG1 and IgE production through the promotion of T_H2 cell responses, although the induction of CD8⁺ T cells by alum has also been reported⁷⁶. For decades, little attention has been given to the immunological mechanisms that drive the adjuvant activity of alum⁷⁷. Renewed interest was sparked by the discovery that alum activates the NLRP3 inflammasome^{78,79}. However, studies on the contribution of NLRP3 to the effects of alum on adaptive immune responses have generated conflicting results^{76,80}, suggesting that the NLRP3 inflammasome is not, in general, essential for the adjuvant activity of alum and that additional mechanisms are involved.

Dead lysed cells have been repeatedly observed at sites of alum injection^{81,82}, implying that alum may induce the release of DAMPs. Research in mouse models recently reported a role for two DAMPs, which were both connected to nucleic acid biology, in the adjuvant activity of alum^{83–85}. Uric acid is the end product of the degradation of purines, and may be rapidly released by injured cells following DNA and RNA degradation. Alum induces the accumulation of uric acid at sites of injection, and reducing uric acid levels *in vivo* through treatment with uricase was shown to inhibit T cell responses and the production of IgG1 and IgE^{83,84}. Uric acid has not been shown to form crystals (its usual form for recognition as a DAMP⁸) at sites of alum injection, and the signalling pathways activated in this context remain to be identified. Alum also induces the rapid release of host cell DNA at sites of injection^{82,85}, and the elimination of extracellular DNA using DNase I treatment decreases alum-induced T cell responses and the production of IgG1 and IgE⁸⁵. Although the PRRs (or PRR) triggered by host DNA in alum immunization were not identified, IRF3 was shown to control the IgE response. However, any contribution of TLRs, RLRs or inflammasomes to this response was ruled out.

Harnessing nucleic acid sensors

With the increased recognition of the impact of nucleic acid-sensing PRRs on APC function, research is well underway to directly harness these PRRs using novel adjuvants. Several candidates, mostly TLR agonists so far, are now in the preclinical or early clinical stages of development⁷⁵.

TLR3 and RLR agonists. The activation of TLR3 in cDCs induces the production of IL-12, type I IFNs and pro-inflammatory cytokines by these cells and upregulates their expression of MHC class II and co-stimulatory molecules, as well as their cross-presentation activity^{86–89}. Of note, cDCs with strong cross-presentation activity — such as CD8 α^+ and CD103⁺ cDCs in mice and DNGR1⁺CD114⁺BDCA3⁺ cDCs in humans — express the highest levels of TLR3 (REFS 88–90).

In preclinical models, co-administration of TLR3 agonists with soluble or DC-targeted antigens was shown to induce durable T_H1 cell^{91–93} and CD8⁺ T cell⁸⁹ responses, as well as augmented antibody responses^{94–95}, which could confer protection against subsequent intracellular pathogen infection^{89,95}.

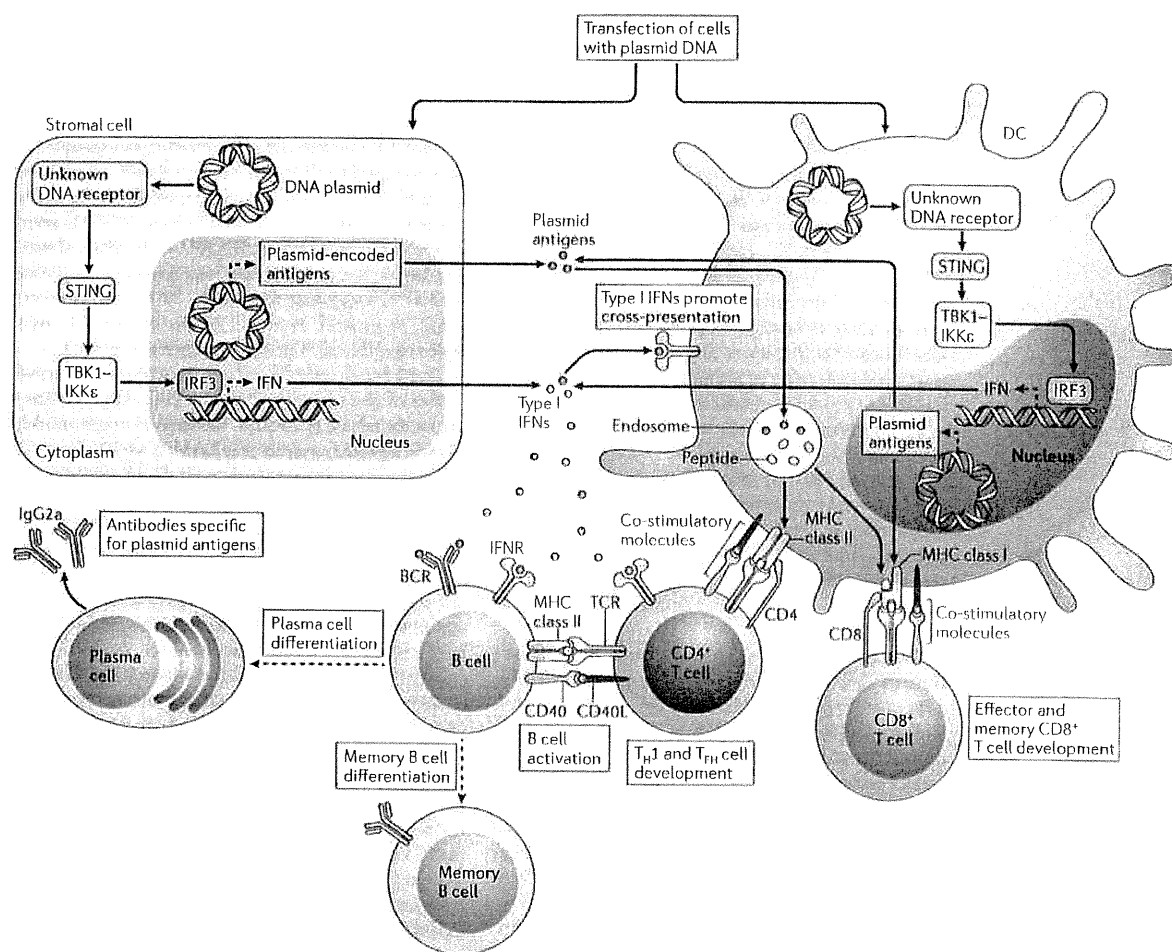


Figure 3 | Mechanisms of DNA vaccination. The plasmid DNA used in DNA vaccination may directly transfect stromal cells (such as muscle cells) or dendritic cells (DCs). In these cells, a cytosolic DNA receptor that has not yet been identified induces the activation of TANK-binding kinase 1 (TBK1) and I κ B kinase- ϵ (IKKe) through stimulator of IFN genes (STING), leading to the activation of interferon-regulatory factor 3 (IRF3) and resulting in the production of type I interferons (IFNs). The antigens encoded by the transfected plasmid DNA can also be expressed in stromal cells and DCs. In DCs, these antigens may be directly processed and presented on MHC class I molecules to naive CD8⁺ T cells. Alternatively, antigens may be indirectly acquired by DCs from stromal cells and then cross-presented to CD8⁺ T cells or presented to naive CD4⁺ T cells on MHC class II molecules. Type I IFN expression by stromal cells and DCs seems to be important for promoting the cross presentation activity of DCs, as well as for the differentiation of T helper 1 (T_H1) cells and the promotion of I_H1-type isotype switching in B cells. BCR, B cell receptor; CD40L, CD40 ligand; TCR, T cell receptor; T_H1, T follicular helper.

Most TLR3 agonists, such as polyI:C, also activate MDA5 in DCs and stromal cells. Both TLR3 and MDA5 were proposed to participate in the induction of type I IFN production^{92,94,96}, which is essential for the development of polyI:C-induced T_H1 and CD8⁺ T cell responses^{92,96}. MDA5-dependent production of type I IFNs by stromal cells seems to be especially important for the generation of memory CD8⁺ T cells in such models⁹⁶. PolyI:C-induced activation of MDA5, but not TLR3, was also shown to be essential for the production of antibodies specific for a co-administered antigen in alum⁹⁴.

Even though the aforementioned immunization studies were performed in mice and nonhuman primates, data are emerging as to the potential adjuvant effects of ligands for TLR3 and MDA5 in humans. As mentioned above, a pilot systems biology study in human subjects compared the innate immune response induced by the YF-17D vaccine to that of an RNase-resistant analogue of polyI:C (polyI:C stabilized with poly-L-lysine and carboxymethylcellulose (polyI:CLC))⁵³. The gene expression profile of blood cells from polyI:CLC-treated subjects showed the induction of a type I IFN response as well as signatures associated with

NF- κ B signalling, inflammasomes and DC activation. However, the response was faster than that observed with YF-17D. TLR3 and MDA5 agonists are thus emerging as promising adjuvants in the development of vaccines that promote a T_H1 -type response against viruses and other intracellular pathogens.

TLR7 and TLR8 agonists. A preferred option to target TLR7 and TLR8 are the small synthetic compounds imidazoquinolines. Given that the expression patterns of TLR7 and TLR8 differ between mice and humans, caution should be exerted when extrapolating results obtained with TLR7 and TLR8 agonists from mice to humans.

In human pDCs, which express TLR7, the activation of this receptor leads to the expression of type I IFNs, IL-12 and pro-inflammatory cytokines, as well as to the upregulation of co-stimulatory molecules^{86,97}. Human cDCs express TLR8, and agonists of this TLR induce the expression of IL-12 and pro-inflammatory cytokines and the upregulation of co-stimulatory molecules^{90,98}.

In mice, the administration of an antigen together with a TLR7 or TLR8 agonist promotes T_H1 and CD8⁺ T cell responses^{99–101} and antibody production⁹⁹. Data from mice and nonhuman primates indicate that conjugation of the TLR7 or TLR8 agonist with the antigen and protein aggregation may result in a more efficient induction of T_H1 and CD8⁺ T cell responses^{102,103}. In mice immunized subcutaneously with an antigen–TLR7/8 agonist conjugate, the improvement in these responses has been attributed to more efficient antigen uptake by multiple DC subsets¹⁰³. TLR7-dependent production of type I IFNs has been implicated in this increased antigen uptake, as well as in the promotion of DC migration to the lymph nodes. Together with IL-12, type I IFNs appear to be required for optimal T_H1 and CD8⁺ T cell responses following the administration of TLR7 and TLR8 agonists^{101,104}. Thus, TLR7 and TLR8 agonists are emerging as promising candidate adjuvants for promoting T_H1 -type immune responses, although the development of improved formulation and delivery strategies is likely to be key for their efficiency in humans.

TLR9 agonists. TLR9 agonists (mostly different types of CpG oligodeoxynucleotides) are the most studied and probably the most advanced nucleic acid-sensing PRR agonists in development as potential immune response-biasing vaccine adjuvants^{75,101}. Again, it should be kept in mind when interpreting rodent studies that TLR9 expression is restricted in humans, being highest in pDCs and B cells, whereas mice have a broader expression pattern¹⁰⁵.

In human pDCs, stimulation of TLR9 leads to strong expression of type I IFNs, IL-12 and pro-inflammatory cytokines, as well as to the upregulation of co-stimulatory molecules⁸⁶. In B cells, TLR9 activation leads to the expression of pro-inflammatory cytokines and, in conjunction with CD40 engagement, synergistically promotes the production of antibodies and IL-12, which allows B cells to promote the differentiation of T_H1 cells¹⁰⁶. Concomitant stimulation of TLR9 in pDCs may further promote B cell antibody production and

memory B cell differentiation in the absence of T cell help through type I IFN production¹⁰⁷. In addition, TLR9 triggering synergizes with B cell receptor activation in the induction of antigen-specific B cell responses and promotes T_H1 -biased isotype switching¹⁰⁸. In mice, TLR9 agonists very potently induce T_H1 and CD8⁺ T cell responses as well as T_H1 -type B cell responses¹⁰⁹.

TLR9 agonists have entered clinical trials as adjuvants in hepatitis B, influenza and anthrax vaccines and have been shown to boost and accelerate protective antibody responses^{75,109}.

STING agonists. The discovery that STING may directly respond to cyclic di-GMP supports the idea that it could be targeted directly by novel adjuvant molecules. So far, this potential can only be inferred from data on cyclic di-GMP, which has immunostimulatory and adjuvant activities that are being increasingly documented¹⁰⁹. For instance, treatment with cyclic di-GMP may upregulate the expression of MHC class II molecules, co-stimulatory molecules, pro-inflammatory cytokines and type I IFNs by human and mouse cDCs^{110,111}. Furthermore, cyclic di-GMP has adjuvant effects on adaptive responses to soluble antigens in mice^{110,111}. It remains to be determined whether the adjuvant activity of cyclic di-GMP *in vivo* is entirely due to STING activation or also a result of other activities of this molecule. Either way, it is likely that STING has an important role, given that mice with an inactivating point mutation in the gene encoding STING display impaired type I IFN responses to cyclic di-GMP¹¹².

Combined adjuvants. In line with the observation that efficient live attenuated vaccines target multiple PRRs^{50,55}, combining multiple PRR agonists appears to be a promising rationale for the design of effective new adjuvants. This approach is already being applied, for instance in the clinically approved adjuvant AS04 (a combination of alum and a TLR4 ligand). Similar strategies aim to couple the potential of nucleic acid-sensing PRRs with that of other PRRs. To date, most studies have combined TLR ligands.

MYD88-dependent and TRIF-dependent TLR ligands synergistically activate cDCs. Thus, a combination of these ligands strongly increases the secretion of IL-12, type I IFNs and pro-inflammatory cytokines by cDCs, resulting in efficient activation of T_H1 cells and CD8⁺ T cells^{113,114}. A recent *in vivo* study in mice using such a combined adjuvant strategy indicated that combining aggregated TLR2–TLR6, TLR3 and TLR9 ligands could boost not only the number of antigen-specific CD8⁺ T cells, but also their avidity and functionality, providing a qualitative advantage over combinations of two agonists¹¹⁵. This difference has been linked to activation of the expression of IL-15 and IL-15 receptor subunit- α (IL-15R α) by cDCs in a type I IFN-dependent manner¹¹⁵. In another study, a TLR4 agonist and a TLR7 agonist, which were combined in nanoparticles, were shown to have synergistic effects in increasing the levels of neutralizing antibodies and promoting the generation of memory B cells and long-lived plasma cells¹¹⁶. These effects were dependent on TLR triggering in

both DCs and B cells, and also on T cell help. Experimental immunizations using this combined adjuvant were shown to protect mice from lethal influenza virus infection and to boost neutralizing antibody responses in nonhuman primates¹¹⁶. Again, such studies highlight the benefit of optimizing formulation and delivery strategies in vaccines containing this type of adjuvant.

Conclusions and perspectives

Nucleic acid-sensing PRRs are taking centre stage in the induction of adaptive immune responses to many existing vaccines. Preclinical and clinical evidence indicates that the triggering of these receptors by selective agonists may suffice in mediating efficient immunization against co-administered antigens. Even though considerable progress has been made in the past decade since the discovery of the first nucleic acid-sensing PRR, much remains to be elucidated concerning the role of these receptors in adaptive immunity in general and in vaccination in particular.

A robust and comprehensive characterization of the nucleic acid-sensing machinery is likely to be key not only to a more complete understanding of antimicrobial immunity, but also for elucidating the mechanisms of action of many current vaccines. For instance, the monopoly of TLR9 on DNA sensing has recently been challenged by the discovery of cytosolic DNA-sensing mechanisms. However, the PRRs that mediate the response to nucleic acids in several important vaccination strategies — including DNA vaccination and alum-adjuvanted immunization — remain to be identified. A few novel DNA- and RNA-sensing PRRs have been proposed using *in vitro* approaches, and we expect that mice (conditionally) deficient for individual nucleic acid sensors should soon help to establish the respective contributions of these PRRs to antimicrobial immunity and vaccination. Moreover, a more advanced characterization of the expression patterns of these receptors and of their ligand-binding specificities could provide new molecular targets for experimental adjuvants or help to optimize delivery strategies. Notably, this could help us to understand the origin of human hypo-responsiveness to DNA vaccines, which deserves more scrutiny.

Another potentially important question is the extent to which host nucleic acids contribute to vaccination, in line with recent data suggesting a role for host DNA and uric acid in mediating the adjuvant effects of alum. In the context of alum-adjuvanted immunization, these

two DAMPs induce T_H2-type responses independently of type I IFNs^{83–85}. This is in contrast to most nucleic acid PAMPs, which induce T_H1-type responses that most often require type I IFN signalling. As it increasingly appears that PRR engagement may result in the active release of host nucleic acids¹¹⁷, we propose that it may be worthwhile studying the potential adjuvant or immunomodulatory effects of host nucleic acids and their metabolites in vaccination. This investigation would probably benefit from the identification of the receptors for uric acid and host DNA that are involved in alum-adjuvanted immunization.

Finally, achieving a more precise understanding of the APCs and the PRRs that are targeted by nucleic acids in different vaccination strategies is likely to be of utmost importance. Indeed, APCs, especially cDCs, are highly heterogeneous, and multiple distinct subsets are present at the various sites potentially used for vaccination and in the lymphoid organs that drain such sites¹¹⁸. The improving characterization of the functional specialization and plasticity of each DC subset provides opportunities for tailoring vaccines to preferentially target specific DC subsets¹¹⁹. Notably in this regard, the expression patterns of intracellular TLRs indicate a distinct distribution among DC subsets that correlates with the functional specialization of each subset^{13,88–90}. It is likely that further characterization of the contribution of pDCs to nucleic acid sensing will be of particular importance. Being 'professional' type I IFN producers, pDCs may at least be important bystander contributors to the triggering of T_H1-type immune responses by nucleic acid sensing in vaccination^{65,120}. Furthermore, recent data suggest that pDCs could directly participate in the activation of CD8⁺ T cells *in vivo*¹²¹, although this notion remains controversial¹²². Determining the main PRRs through which pDCs react to nucleic acids in different settings could also provide valuable information. Although most research to date has focused on TLRs, there is evidence, for instance, that pDCs may respond to immunostimulatory dsDNA via STING⁷¹. Emerging mouse models that allow for the deletion of specific DC subsets or of genes encoding nucleic acid-sensing PRRs within these subsets are likely to help in deconstructing the relative contributions of pDCs and other DC subsets in the immune responses to different vaccines. This knowledge could be key to refining the formulation and delivery strategies for new vaccine adjuvants tailored to elicit specific types of adaptive immune response.

- Coffman, R. L., Sher, A. & Seder, R. A. Vaccine adjuvants: putting innate immunity to work. *Immunity* **33**, 492–503 (2010)
- Pulendran, B. & Ahmed, R. Immunological mechanisms of vaccination. *Nature Immunol.* **13**, 509–517 (2011)
- Plotkin, S. A. Vaccines: correlates of vaccine-induced immunity. *Clin. Infect. Dis.* **47**, 401–409 (2008)
- Iwasaki, A. & Medzhitov, R. Regulation of adaptive immunity by the innate immune system. *Science* **327**, 291–295 (2010)
- Pichlmair, A. & Reis e Sousa, C. Innate recognition of viruses. *Immunity* **27**, 370–383 (2007)
- Takeuchi, O. & Akira, S. Pattern recognition receptors and inflammation. *Cell* **140**, 805–820 (2010)
- Barbalat, R., Ewald, S. E., Mouchess, M. L. & Barton, G. M. Nucleic acid recognition by the innate immune system. *Annu. Rev. Immunol.* **29**, 185–214 (2011)
- Chen, G. Y. & Nunez, G. Sterile inflammation: sensing and reacting to damage. *Nature Rev. Immunol.* **10**, 826–837 (2010)
- Blasius, A. L. & Beutler, B. Intracellular Toll-like receptors. *Immunity* **32**, 305–315 (2010)
- Kawai, T. & Akira, S. Toll-like receptors and their crosstalk with other innate receptors in infection and immunity. *Immunity* **34**, 637–650 (2011)
- Loo, Y. M. & Gale, M. Jr. Immune signaling by RIG-I-like receptors. *Immunity* **34**, 680–692 (2011)
- Kadowaki, N. *et al.* Subsets of human dendritic cell precursors express different Toll-like receptors and respond to different microbial antigens. *J. Exp. Med.* **194**, 863–869 (2001)
- Iwasaki, A. & Medzhitov, R. Toll-like receptor control of the adaptive immune responses. *Nature Immunol.* **5**, 987–995 (2004)
- Kawai, T. & Akira, S. The role of pattern-recognition receptors in innate immunity: update on Toll-like receptors. *Nature Immunol.* **11**, 373–384 (2010)
- Schlee, M. & Hartmann, G. The chase for the RIG-I ligand — recent advances. *Mol. Ther.* **18**, 1254–1262 (2010)
- Ablasser, A. *et al.* RIG-I-dependent sensing of poly(dA:dT) through the induction of an RNA polymerase III-transcribed RNA intermediate. *Nature Immunol.* **10**, 1065–1072 (2009)

REVIEWS

- 17 Chiu, Y.-H., MacMillan, J. B. & Chen, Z. J. RNA polymerase III detects cytosolic DNA and induces type I interferons through the RIG-I pathway. *Cell* **138**, 576–591 (2009)
- 18 Kato, H. *et al.* Length-dependent recognition of double-stranded ribonucleic acids by retinoic acid-inducible gene-1 and melanoma differentiation-associated gene 5. *J. Exp. Med.* **205**, 1601–1610 (2008)
- 19 Malathi, K., Dong, B., Gale, M. & Silverman, R. H. Small self-RNA generated by RNase L amplifies antiviral innate immunity. *Nature* **448**, 816–819 (2007)
- 20 Venkataraman, T. *et al.* Loss of DEX/DH box RNA helicase IGP2 manifests disparate antiviral responses. *J. Immunol.* **178**, 6444–6455 (2007)
- 21 Satoh, T. *et al.* IGP2 is a positive regulator of RIG-I and MDA5-mediated antiviral responses. *Proc. Natl. Acad. Sci. USA* **107**, 1512–1517 (2010)
- 22 Monroe, K. M., McWhirter, S. M. & Vance, R. E. Identification of host cytosolic sensors and bacterial factors regulating the type I interferon response to *Legionella pneumophila*. *PLoS Pathog.* **5**, e1000665 (2009)
- 23 Li, X. D. *et al.* Mitochondrial antiviral signaling protein (MAVS) monitors commensal bacteria and induces an immune response that prevents experimental colitis. *Proc. Natl. Acad. Sci. USA* **108**, 17390–17395 (2011)
- 24 Poock, H. *et al.* Recognition of RNA virus by RIG-I results in activation of CARD9 and inflammasome signaling for interleukin 1 β production. *Nature Immunol.* **11**, 63–69 (2010)
- 25 Ishikawa, H. & Barber, G. N. STING is an endoplasmic reticulum adaptor that facilitates innate immune signalling. *Nature* **455**, 674–678 (2008)
- 26 Zhong, B. *et al.* The adaptor protein MITA links virus-sensing receptors to IRF-3 transcription factor activation. *Immunity* **29**, 558–550 (2008)
- 27 Oshiumi, H., Sakai, K., Matsumoto, M. & Seya, T. DEAD/H BOX 5 (DDX5) helicase binds the RIG-I adaptor IPS-1 to up-regulate IFN- β -inducing potential. *Eur. J. Immunol.* **40**, 940–948 (2010)
- 28 Zhang, Z. *et al.* DDX1, DDX21, and DHX56 helicases form a complex with the adaptor molecule TRIF to sense dsRNA in dendritic cells. *Immunity* **34**, 866–878 (2011)
- 29 Miyashita, M., Oshiumi, H., Matsumoto, M. & Seya, T. DDX60, a DF XD/H box helicase, is a novel antiviral factor promoting RIG-I-like receptor-mediated signaling. *Mol. Cell. Biol.* **31**, 3802–3819 (2011)
- 30 Kim, T. *et al.* Aspartate-glutamate-alanine-histidine box motif (DEAH) RNA helicase A helicases sense microbial DNA in human plasmacytoid dendritic cells. *Proc. Natl. Acad. Sci. USA* **107**, 15181–15186 (2010)
- 31 Zhang, Z. *et al.* The helicase DDX41 senses intracellular DNA mediated by the adaptor STING in dendritic cells. *Nature Immunol.* **12**, 959–965 (2011)
- 32 Zhang, Z., Yuan, B., Lu, N., Facchinetti, V. & Liu, Y. J. DHX9 pairs with IPS-1 to sense double-stranded RNA in myeloid dendritic cells. *J. Immunol.* **187**, 4501–4508 (2011)
- 33 Elinav, E., Strowig, T., Henao-Mejia, J. & Flavell, R. A. Regulation of the antimicrobial response by NLR proteins. *Immunity* **34**, 665–679 (2011)
- 34 Sabbah, A. *et al.* Activation of innate immune antiviral responses by Nod2. *Nature Immunol.* **10**, 1075–1080 (2009)
- 35 Kanneganti, T. D. *et al.* Critical role for *Cryopyrin*/Nalp3 in activation of caspase-1 in response to viral infection and double-stranded RNA. *J. Biol. Chem.* **281**, 56560–56568 (2006)
- 36 Allen, I. C. *et al.* The NLRP3 inflammasome mediates *in vivo* innate immunity to influenza A virus through recognition of viral RNA. *Immunity* **30**, 556–565 (2009)
- 37 Shimada, K. *et al.* Oxidized mitochondrial DNA activates the NLRP3 inflammasome during apoptosis. *Immunity* **36**, 401–414 (2012)
- 38 Keating, S. E., Baran, M. & Bowie, A. G. Cytosolic DNA sensors regulating type I interferon induction. *Trends Immunol.* **32**, 574–581 (2011)
- 39 Burckstummer, T. *et al.* An orthogonal proteomic-screen identifies AIM2 as a cytoplasmic DNA sensor for the inflammasome. *Nature Immunol.* **10**, 266–272 (2009)
- 40 Fernandes-Alnemri, T., Yu, J.-W., Datta, P., Wu, J. & Alnemri, E. S. AIM2 activates the inflammasome and cell death in response to cytoplasmic DNA. *Nature* **458**, 509–515 (2009)
- 41 Hörnung, V. *et al.* AIM2 recognizes cytosolic dsDNA and forms a caspase-1-activating inflammasome with ASC. *Nature* **458**, 514–518 (2009)
- 42 Roberts, T. L. *et al.* HIN-200 proteins regulate caspase activation in response to foreign cytoplasmic DNA. *Science* **323**, 1057–1060 (2009)
- 43 Unterholzner, L. *et al.* IFI16 is an innate immune sensor for intracellular DNA. *Nature Immunol.* **11**, 997–1004 (2010)
- 44 Kerur, N. *et al.* IFI16 acts as a nuclear pathogen sensor to induce the inflammasome in response to Kaposi sarcoma-associated herpesvirus infection. *Cell Host Microbe* **9**, 363–375 (2011)
- 45 Takaoka, A. *et al.* DAI (DLM-1/ZBP1) is a cytosolic DNA sensor and an activator of innate immune response. *Nature* **448**, 501–505 (2007)
- 46 Kaiser, W. J., Upton, J. W. & Muranski, E. S. Receptor-interacting protein homotypic interaction motif-dependent control of NF- κ B activation via the DNA-dependent activator of IFN regulatory factors. *J. Immunol.* **181**, 6421–6434 (2008)
- 47 Ishii, K. J. *et al.* TANK-binding kinase-1 delineates innate and adaptive immune responses to DNA vaccines. *Nature* **451**, 725–729 (2008)
- 48 Yang, P. *et al.* The cytosolic nucleic acid sensor LRRFIP1 mediates the production of type I interferon via a β -catenin-dependent pathway. *Nature Immunol.* **11**, 487–494 (2010)
- 49 Burdette, D. L. *et al.* STING is a direct innate immune sensor of cyclic di-GMP. *Nature* **478**, 515–518 (2011)
- 50 Querec, T. *et al.* Yellow fever vaccine YF-17D activates multiple dendritic cell subsets via TLR2, 7, 8, and 9 to stimulate polyvalent immunity. *J. Exp. Med.* **203**, 413–424 (2006)
- 51 Gaucher, D. *et al.* Yellow fever vaccine induces integrated multilineage and polyfunctional immune responses. *J. Exp. Med.* **205**, 3119–3131 (2008)
- 52 Querec, T. D. *et al.* Systems biology approach predicts immunogenicity of the yellow fever vaccine in humans. *Nature Immunol.* **10**, 116–125 (2009)
- 53 Caskey, M. *et al.* Synthetic double-stranded RNA induces innate immune responses similar to a live viral vaccine in humans. *J. Exp. Med.* **208**, 2357–2366 (2011). References 51–53 illustrate how systems biology may help to deconstruct the mechanisms of action of current vaccines in humans.
- 54 Samuelsson, C. *et al.* Survival of lethal poxvirus infection in mice depends on TLR9, and therapeutic vaccination provides protection. *J. Clin. Invest.* **118**, 1776–1784 (2008)
- 55 Delaloye, J. *et al.* Innate immune sensing of modified vaccinia virus Ankara (MVA) is mediated by TLR2-IL1R6, MDA-5 and the NALP3 inflammasome. *PLoS Pathog.* **5**, e1000480 (2009)
- 56 Zhu, J., Martinez, J., Huang, X. & Yang, Y. Innate immunity against vaccinia virus is mediated by TLR2 and requires TLR-independent production of IFN- β . *Blood* **109**, 619–625 (2007)
- 57 Quigley, M., Martinez, J., Huang, X. & Yang, Y. A critical role for direct TLR2-MyD88 signaling in CD8⁺ T-cell clonal expansion and memory formation following vaccinia viral infection. *Blood* **113**, 2256–2264 (2009)
- 58 Martinez, J., Huang, X. & Yang, Y. Toll-like receptor 2-mediated activation of murine plasmacytoid dendritic cells by vaccinia viral DNA. *Proc. Natl. Acad. Sci. USA* **107**, 6442–6447 (2010)
- 59 Diebold, S. S., Kishino, T., Hemmi, H., Akira, S. & Reis e Sousa, C. Innate antiviral responses by means of TLR7-mediated recognition of single-stranded RNA. *Science* **303**, 1529–1531 (2004)
- 60 Lund, J. M. *et al.* Recognition of single-stranded RNA viruses by Toll-like receptor 7. *Proc. Natl. Acad. Sci. USA* **101**, 5598–5605 (2004)
- 61 Yoneyama, M. *et al.* The RNA helicase RIG-I has an essential function in double-stranded RNA-induced innate antiviral responses. *Nature Immunol.* **5**, 730–737 (2004)
- 62 Kato, H. *et al.* Cell type-specific involvement of RIG-I in antiviral response. *Immunity* **23**, 19–28 (2005)
- 63 Thomas, P. G. *et al.* The intracellular sensor NLRP3 mediates key innate and healing responses to influenza A virus via the regulation of caspase-1. *Immunity* **30**, 566–575 (2009)
- 64 Koyama, S. *et al.* Plasmacytoid dendritic cells delineate immunogenicity of influenza vaccine subtypes. *Sci. Transl. Med.* **2**, 251a24 (2010)
- 65 Aoshi, T., Koyama, S., Kobiyama, K., Akira, S. & Ishii, K. J. Innate and adaptive immune responses to viral infection and vaccination. *Curr. Opin. Virol.* **1**, 226–232 (2011)
- 66 Mancuso, G. *et al.* Bacterial recognition by TLR7 in the lysosomes of conventional dendritic cells. *Nature Immunol.* **10**, 587–594 (2009)
- 67 von Meyenn, F. *et al.* Toll-like receptor 9 contributes to recognition of *Mycobacterium bovis* Bacillus Calmette-Guérin by Flt3-ligand generated dendritic cells. *Immunobiology* **211**, 557–565 (2006)
- 68 Sander, L. E. *et al.* Detection of prokaryotic mRNA signifies microbial viability and promotes immunity. *Nature* **474**, 385–389 (2011). This study supports the idea that bacterial nucleic acids may be recognized as a signal of microbial viability and may contribute to an enhanced adaptive immune response against the pathogen.
- 69 Liu, M. A. Immunologic basis of vaccine vectors. *Immunity* **33**, 504–515 (2010)
- 70 Coban, C. *et al.* Novel strategies to improve DNA vaccine immunogenicity. *Curr. Gene Ther.* **11**, 479–484 (2011)
- 71 Spies, B. *et al.* Vaccination with plasmid DNA activates dendritic cells via Toll-like receptor 9 (TLR9) but functions in TLR9-deficient mice. *J. Immunol.* **171**, 5908–5912 (2005)
- 72 Babiuk, S. *et al.* TLR9^{-/-} and TLR9^{+/+} mice display similar immune responses to a DNA vaccine. *Immunology* **113**, 114–120 (2004)
- 73 Rottembourg, D. *et al.* Essential role for TLR9 in prime but not prime-boost plasmid DNA vaccination to activate dendritic cells and protect from lethal viral infection. *J. Immunol.* **184**, 7100–7107 (2010)
- 74 Ishikawa, H., Ma, Z. & Barber, G. N. STING regulates intracellular DNA-mediated, type I interferon-dependent innate immunity. *Nature* **461**, 788–792 (2009). This study identifies STING as an essential adaptor protein in the signalling pathways of TBK1-activating cytosolic DNA sensors.
- 75 Mbaw, M. L., De Gregorio, E., Valiante, N. M. & Rappuoli, R. New adjuvants for human vaccines. *Curr. Opin. Immunol.* **22**, 411–416 (2010)
- 76 McKee, A. S. *et al.* Alum induces innate immune responses through macrophage and mast cell sensors, but these sensors are not required for alum to act as an adjuvant for specific immunity. *J. Immunol.* **183**, 4403–4414 (2009)
- 77 Marrack, P., McKee, A. S. & Munks, M. W. Towards an understanding of the adjuvant action of aluminium. *Nature Rev. Immunol.* **9**, 287–293 (2009)
- 78 Hörnung, V. *et al.* Silica crystals and aluminium salts activate the NALP3 inflammasome through phagosomal destabilization. *Nature Immunol.* **9**, 847–856 (2008)
- 79 Eisenbarth, S. C., Colegio, O. R., O'Connor, W., Sutterwala, F. S. & Flavell, R. A. Crucial role for the Nalp3 inflammasome in the immunostimulatory properties of aluminium adjuvants. *Nature* **453**, 1122–1126 (2008)
- 80 Spreafico, R., Riccardi-Castagnoli, P. & Mortellaro, A. The controversial relationship between NLRP3, alum, danger signals and the next-generation adjuvants. *Eur. J. Immunol.* **40**, 658–662 (2010)
- 81 Goto, N. *et al.* Local tissue irritating effects and adjuvant activities of calcium phosphate and aluminium hydroxide with different physical properties. *Vaccine* **15**, 1364–1371 (1997)
- 82 Munks, M. W. *et al.* Aluminium adjuvants elicit fibrin-dependent extracellular traps *in vivo*. *Blood* **116**, 5191–5199 (2010)
- 83 Kool, M. *et al.* Alum adjuvant boosts adaptive immunity by inducing uric acid and activating inflammatory dendritic cells. *J. Exp. Med.* **205**, 869–882 (2008)
- 84 Kool, M. *et al.* An unexpected role for uric acid as an inducer of T helper 2 cell immunity to inhaled antigens and inflammatory mediator of allergic asthma. *Immunity* **34**, 577–540 (2011)
- 85 Marichal, T. *et al.* DNA released from dying host cells mediates aluminium adjuvant activity. *Nature Med.* **17**, 996–1002 (2011)
- 86 Lore, K. *et al.* Toll-like receptor ligands modulate dendritic cells to augment cytomegalovirus- and HIV-1-specific T cell responses. *J. Immunol.* **171**, 4320–4328 (2003)
- 87 Schulz, O. *et al.* Toll-like receptor 3 promotes cross-priming to virus-infected cells. *Nature* **433**, 881–892 (2005)
- 88 Jongbloed, S. L. *et al.* Human CD141⁺ (BDCA-3)⁺ dendritic cells (DCs) represent a unique myeloid DC subset that cross-presents necrotic cell antigens. *J. Exp. Med.* **207**, 1247–1260 (2010)

- 83 Jelinek, I. *et al.* TLR3-specific double-stranded RNA oligonucleotide adjuvants induce dendritic cell cross-presentation, CTL responses, and antiviral protection. *J. Immunol.* **186**, 2422–2429 (2011).
- 90 Poulin, L. F. *et al.* Characterization of human DNGR-1⁺ BDCA3⁺ leukocytes as putative equivalents of mouse CD8a⁺ dendritic cells. *J. Exp. Med.* **207**, 1261–1271 (2010).
- 91 Trunpfheller, C. *et al.* The microbial mimic poly I:C induces durable and protective CD4⁺ T cell immunity together with a dendritic cell targeted vaccine. *Proc. Natl Acad. Sci. USA* **105**, 2574–2579 (2008).
- 92 Longhi, M. P. *et al.* Dendritic cells require a systemic type I interferon response to mature and induce CD4⁺ Th1 immunity with poly I:C as adjuvant. *J. Exp. Med.* **206**, 1589–1602 (2009).
- 93 Stahl-Hennig, C. *et al.* Synthetic double-stranded RNAs are adjuvants for the induction of T helper 1 and humoral immune responses to human papillomavirus in rhesus macaques. *PLoS Pathog.* **5**, e1000373 (2009).
- 94 Kumar, H., Koyama, S., Ishii, K. J., Kawai, T. & Akira, S. Cutting edge: cooperation of IPS-1- and TRIF-dependent pathways in poly I:C-enhanced antibody production and cytotoxic T cell responses. *J. Immunol.* **180**, 683–687 (2008).
- 95 Tewari, K. *et al.* Poly(I:C) is an effective adjuvant for antibody and multi-functional CD4⁺ T cell responses to *Plasmodium falciparum* circumsporozoite protein (CSP) and aDEC-CSP in non human primates. *Vaccine* **28**, 7256–7266 (2010).
- 96 Wang, Y., Cella, M., Gillfillan, S. & Colonna, M. Cutting edge: polyinosinic:polycytidylic acid boosts the generation of memory CD8 T cells through melanoma differentiation-associated protein 5 expressed in stromal cells. *J. Immunol.* **184**, 2751–2755 (2010).
- 97 Russo, C. *et al.* Small molecule Toll-like receptor 7 agonists localize to the MHC class II loading compartment of human plasmacytoid dendritic cells. *Blood* **117**, 5683–5691 (2011).
- 98 Levy, O., Suter, E. E., Miller, R. L. & Wessels, M. R. Unique efficacy of Toll-like receptor 8 agonists in activating human neonatal antigen-presenting cells. *Blood* **108**, 1284–1290 (2006).
- 99 Hamm, S. *et al.* Immunostimulatory RNA is a potent inducer of antigen-specific cytotoxic and humoral immune response *in vivo*. *Int. Immunol.* **19**, 297–304 (2007).
- 100 Zhang, W. W. & Mattshewski, G. Immunization with a Toll-like receptor 7 and/or 8 agonist vaccine adjuvant increases protective immunity against *Leishmania major* in BALB/c mice. *Infect. Immun.* **76**, 3777–3783 (2008).
- 101 Rajagopal, D. *et al.* Plasmacytoid dendritic cell-derived type I interferon is crucial for the adjuvant activity of Toll-like receptor 7 agonists. *Blood* **115**, 1949–1957 (2010).
- 102 Wille-Reece, U. *et al.* HIV Gag protein conjugated to a Toll-like receptor 7/8 agonist improves the magnitude and quality of Th1 and CD8⁺ T cell responses in nonhuman primates. *Proc. Natl Acad. Sci. USA* **102**, 15190–15194 (2005).
- 103 Kastenmuller, K. *et al.* Protective T cell immunity in mice following protein-TLR7/8 agonist-conjugate immunization requires aggregation, type I IFN, and multiple DC subsets. *J. Clin. Invest.* **121**, 1782–1796 (2011).
- References 102 and 103 show how optimizing the formulation of agonists for nucleic acid sensors may affect quantitative and qualitative aspects of the response to subunit vaccines adjuvanted with such molecules.
- 104 Huang, X. & Yang, Y. Targeting the TLR9–MyD88 pathway in the regulation of adaptive immune responses. *Expert Opin. Ther. Targets* **14**, 787–796 (2010).
- 105 Campbell, J. D. *et al.* CpG-containing immunostimulatory DNA sequences elicit TNF- α -dependent toxicity in rodents but not in humans. *J. Clin. Invest.* **119**, 2564–2576 (2009).
- 106 Wagner, M. *et al.* IL-12p70-dependent Th1 induction by human B cells requires combined activation with CD40 ligand and CpG DNA. *J. Immunol.* **172**, 954–963 (2004).
- 107 Poeck, H. *et al.* Plasmacytoid dendritic cells, antigen, and CpG-C license human B cells for plasma cell differentiation and immunoglobulin production in the absence of T-cell help. *Blood* **103**, 3058–3064 (2004).
- 108 Krieg, A. M. *et al.* CpG motifs in bacterial DNA trigger direct B-cell activation. *Nature* **374**, 546–549 (1995).
- 109 Chen, W., Kwole, R. & Yan, H. The potential of 3',5'-cyclic diguanylic acid (c-di-GMP) as an effective vaccine adjuvant. *Vaccine* **28**, 3080–3085 (2010).
- 110 Karaolis, D. K. *et al.* Bacterial c-di-GMP is an immunostimulatory molecule. *J. Immunol.* **178**, 2171–2181 (2007).
- 111 McWhirter, S. M. *et al.* A host type I interferon response is induced by cytosolic sensing of the bacterial second messenger cyclic-di-GMP. *J. Exp. Med.* **206**, 1899–1911 (2009).
- 112 Sauer, J. D. *et al.* The *N*-methyl-*N*-nitrosourea-induced Goldenlicket mouse mutant reveals an essential function of Sting in the *in vivo* interferon response to *Listeria monocytogenes* and cyclic dinucleotides. *Infect. Immun.* **79**, 688–694 (2011).
- 113 Trinchieri, G. & Sher, A. Cooperation of Toll-like receptor signals in innate immune defence. *Nature Rev. Immunol.* **7**, 179–190 (2007).
- 114 Zhu, O. *et al.* Toll-like receptor ligands synergize through distinct dendritic cell pathways to induce T cell responses: implications for vaccines. *Proc. Natl Acad. Sci. USA* **105**, 16260–16265 (2008).
- 115 Zhu, O. *et al.* Using 3 TLR ligands as a combination adjuvant induces qualitative changes in T cell responses needed for antiviral protection in mice. *J. Clin. Invest.* **120**, 607–616 (2010).
- 116 Kasturi, S. P. *et al.* Programming the magnitude and persistence of antibody responses with innate immunity. *Nature* **470**, 543–547 (2011).
- References 115 and 116 illustrate how combining nucleic acid sensor agonists and optimizing their delivery strategies could allow fine-tuning of the responses to subunit vaccines.
- 117 Remijsen, O. *et al.* Dying for a cause: NETosis, mechanisms behind an antimicrobial cell death modality. *Cell Death Differ.* **18**, 581–588 (2011).
- 118 Hashimoto, D., Miller, J. & Merad, M. Dendritic cell and macrophage heterogeneity *in vivo*. *Immunity* **35**, 323–335 (2011).
- 119 Palucka, K., Banchereau, J. & Mellman, I. Designing vaccines based on biology of human dendritic cell subsets. *Immunity* **33**, 464–478 (2010).
- 120 Gillet, M., Cao, W. & Liu, Y.-J. Plasmacytoid dendritic cells: sensing nucleic acids in viral infection and autoimmune diseases. *Nature Rev. Immunol.* **8**, 594–606 (2008).
- 121 Takagi, H. *et al.* Plasmacytoid dendritic cells are crucial for the initiation of inflammation and T cell immunity *in vivo*. *Immunity* **35**, 958–971 (2011). This study suggests a direct role of pDCs in the priming of CD8⁺ T cell responses *in vivo*.
- 122 Reizis, B., Colonna, M., Trinchieri, G., Barral, F. & Gillet, M. Plasmacytoid dendritic cells: one-trick ponies or workhorses of the immune system? *Nature Rev. Immunol.* **11**, 558–565 (2011).
- 123 Janeway, C. A. Jr. Approaching the asymptote? Evolution and revolution in immunology. *Cold Spring Harb. Symp. Quant. Biol.* **54** (Pt 1), 1–13 (1989).
- 124 Matzinger, P. Tolerance, danger, and the extended family. *Annu. Rev. Immunol.* **12**, 991–1045 (1994).
- 125 González-Navajas, J. M., Lee, J., David, M. & Raz, E. Immunomodulatory functions of type I interferons. *Nature Rev. Immunol.* **12**, 125–135 (2012).
- 126 Sadler, A. J. & Williams, B. R. Interferon-inducible antiviral effectors. *Nature Rev. Immunol.* **8**, 559–568 (2008).

Acknowledgements

The authors thank F. Bureau, C. Cohan and T. Marichal for critical reading of the manuscript. C.J.D. is supported by the Fonds National de la Recherche Scientifique (FRS-FNRS, Belgium; Fonds pour la Recherche Scientifique Médicale grant). K.J.I. is supported by a Health and Labour Sciences Research Grant of the Japanese Ministry of Health, Labour and Welfare and by the Core Research Evolutionary Science and Technology (CREST) programme at the Japan Science and Technology Agency.

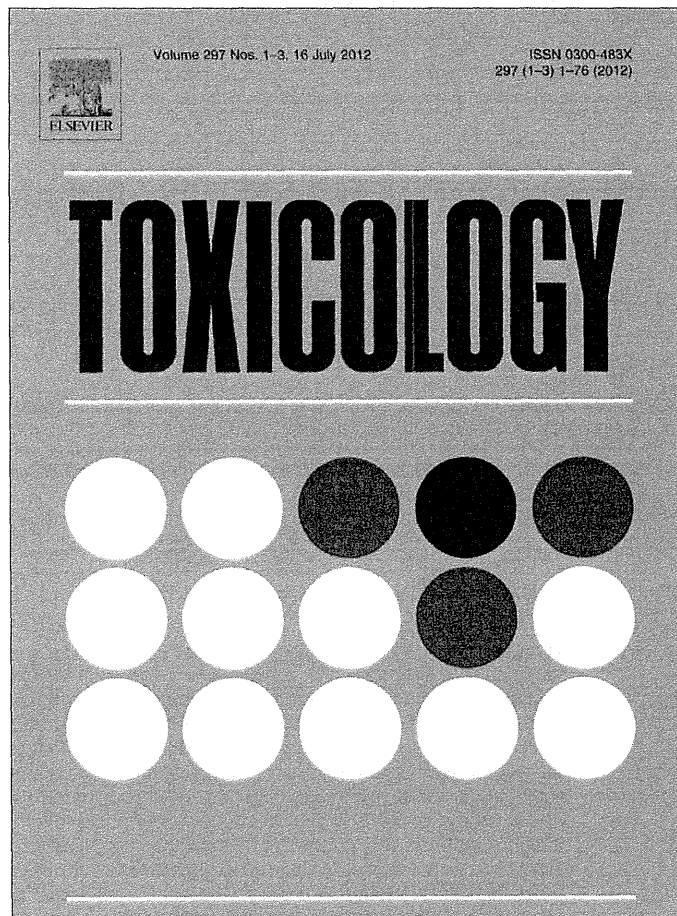
Competing interests statement

The authors declare no competing financial interests.

FURTHER INFORMATION

Christophe J. Desmet's homepage: <http://www.giga.ulg.ac.be/~pcn>
Ken J. Ishii's homepage: <http://www.wilrec.osaka-u.ac.jp/en/laboratory/vaccinescience/index.php>
ALL LINKS ARE ACTIVE IN THE ONLINE PDF

Provided for non-commercial research and education use.
Not for reproduction, distribution or commercial use.

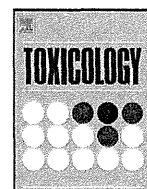


This article appeared in a journal published by Elsevier. The attached copy is furnished to the author for internal non-commercial research and education use, including for instruction at the authors institution and sharing with colleagues.

Other uses, including reproduction and distribution, or selling or licensing copies, or posting to personal, institutional or third party websites are prohibited.

In most cases authors are permitted to post their version of the article (e.g. in Word or Tex form) to their personal website or institutional repository. Authors requiring further information regarding Elsevier's archiving and manuscript policies are encouraged to visit:

<http://www.elsevier.com/copyright>



Toxicogenomic multigene biomarker for predicting the future onset of proximal tubular injury in rats

Yohsuke Minowa^{a,*,1}, Chiaki Kondo^{b,1}, Takeki Uehara^{a,b,c,*,1}, Yuji Morikawa^a, Yasushi Okuno^d, Noriyuki Nakatsu^a, Atsushi Ono^a, Toshiyuki Maruyama^b, Ikuo Kato^b, Jyoji Yamate^c, Hiroshi Yamada^a, Yasuo Ohno^e, Tetsuro Urushidani^f

^a Toxicogenomics-Informatics Project, National Institute of Biomedical Innovation, 7-6-8 Asagi Saito, Ibaraki, Osaka 567-0085, Japan

^b Drug Developmental Research Laboratories, Shionogi & Co., Ltd., 3-1-1, Futaba-cho, Toyonaka, Osaka, Japan

^c Veterinary Pathology, Graduate School of Life and Environmental Sciences, Osaka Prefecture University, 1-58, Rinku-ourai-kita, Izumisano City, Osaka 598-8531, Japan

^d Department of Systems Bioscience for Drug Discovery, Graduate School of Pharmaceutical Sciences, Kyoto University, 46-29, Yoshida Shimoadachi-cho, Kyoto 606-8501, Japan

^e National Institute of Health Sciences, Kamiyoga 1-18-1, Setagaya-ku, Tokyo 158-8501, Japan

^f Department of Pathophysiology, Faculty of Pharmaceutical Sciences, Doshisha Women's College of Liberal Arts, Kodo, Kyotanabe, Kyoto 610-0395, Japan

ARTICLE INFO

Article history:

Received 9 March 2012

Received in revised form 28 March 2012

Accepted 30 March 2012

Available online 6 April 2012

Keywords:

Microarray

Toxicogenomics

Kidney

Nephrotoxicity

Proximal tubular injury

Rat

ABSTRACT

Drug-induced renal tubular injury is a major concern in the preclinical safety evaluation of drug candidates. Toxicogenomics is now a generally accepted tool for identifying chemicals with potential safety problems. The specific aim of the present study was to develop a model for use in predicting the future onset of drug-induced proximal tubular injury following repeated dosing with various nephrotoxicants. In total, 41 nephrotoxic and nonnephrotoxic compounds were used for the present analysis. Male Sprague-Dawley rats were dosed orally or intravenously once daily. Animals were exposed to three different doses (low, middle, and high) of each compound, and kidney tissue was collected at 3, 6, 9, and 24 h after single dosing, and on days 4, 8, 15, and 29 after repeated dosing. Gene expression profiles were generated from kidney total RNA using Affymetrix DNA microarrays. Filter-type gene selection and linear classification algorithms were employed to discriminate future onset of proximal tubular injury. We identified genomic biomarkers for use in future onset prediction using the gene expression profiles determined on day 1, when most of the nephrotoxicants had yet to produce detectable histopathological changes. The model was evaluated using a five-fold cross validation, and achieved a sensitivity of 93% and selectivity of 90% with 19 probes. We also found that the prediction accuracy of the optimized model was substantially higher than that produced by any of the single genomic biomarkers or histopathology. The genes included in our model were primarily involved in DNA replication, cell cycle control, apoptosis, and responses to oxidative stress and chemical stimuli. In summary, our toxicogenomic model is particularly useful for predicting the future onset of proximal tubular injury.

© 2012 Elsevier Ireland Ltd. All rights reserved.

1. Introduction

The kidney is a major organ for the filtration, secretion, reabsorption, and ultimate excretion of drugs and drug metabolites. Nephrotoxicity frequently occurs following administration of various drugs or exposure to xenobiotics. The proximal tubular cells of the kidney are particularly vulnerable to drug-induced injury, and

thus proximal tubular toxicity is a significant concern in the preclinical safety evaluation of candidate drugs. A number of recent studies have illustrated the use of microarray gene expression analyses for preclinical prediction and diagnosis of renal tubular toxicity (Amin et al., 2004; Fielden et al., 2005; Huang et al., 2001; Jiang et al., 2007; Kondo et al., 2009; Thukral et al., 2005). However, when biomarkers and/or classification models based on gene expression data are intended for broad research or regulatory use, the size and diversity of the modeling training set must be considered (Goodsaid et al., 2009). In addition, large-scale validation of biomarkers using external data sets are required (Ransohoff, 2004; Somorjai et al., 2003).

A large-scale toxicogenomics database containing data from multiple time points and dose levels would be useful in the identification and validation of markers of nephrotoxicity. Such a database should facilitate identification of robust biomarker genes

* Corresponding author at: Drug Developmental Research Laboratories, Shionogi & Co., Ltd., 3-1-1, Futaba-cho, Toyonaka, Osaka, Japan. Tel.: +81 6 6331 8195; fax: +81 6 6332 6385.

** Corresponding author. Tel.: +81 72 641 9826; fax: +81 72 641 9850.

E-mail addresses: yminowa@nibio.go.jp (Y. Minowa),

takeki.uehara@shionogi.co.jp (T. Uehara).

¹ These authors equally contributed to this work.

and enable researchers to more easily assess hypotheses generated in previous studies that involved comparatively smaller data sets. In Japan, the Toxicogenomics Project (TGP) developed just such a large-scale toxicogenomics database, known as the Genomics-Assisted Toxicity Evaluation System (TG-GATES) (Uehara et al., 2010; Urushidani and Nagao, 2005; Urushidani, 2010). Using microarrays, the TGP comprehensively analyzed gene expression in the liver and kidney of rats treated with 150 select compounds at three different doses and eight different time points. The resulting database was used to identify a number of biomarker genes and develop prediction models for the hepatotoxicity and nephrotoxicity of the selected compounds (Gao et al., 2010; Hirode et al., 2008, 2009; Kondo et al., 2009; Uehara et al., 2008, 2010, 2011). Among the 150 compounds examined in the TGP study, 13 (including cisplatin, carboplatin, cyclosporine A, gentamicin, and phenacetin) are typical nephrotoxics or drugs for which there is both clinical and nonclinical evidence of nephrotoxicity, while 20 compounds (including phenylbutazone, ethionine, and indomethacin) exhibited both nephrotoxicity and hepatotoxicity in our 28-day repeated-dosing study in rats. In the present study, we comprehensively examined the profile of gene expression in the kidney after exposure to 33 nephrotoxics and eight non-nephrotoxic negative control compounds. The gene expression data obtained from analysis of these 41 compounds are currently available in the open TG-GATES database (<http://toxico.nibio.go.jp/>) for use in nephrotoxicological studies.

Several recent reports have focused on genomic biomarkers of nephrotoxicity in rats. Recently, we constructed a toxicogenomic model for diagnosis of renal tubular injury using microarray data in repeated-dose studies (Kondo et al., 2009). This model consisted of 92 different probes and achieved a sensitivity of 93% and selectivity of 90% in the detection of renal tubular injury following repeated doses of nephrotoxics. Although this model is useful for diagnosis of renal tubular injury in the repeated-dose studies, there remains a need to develop additional toxicogenomics-based biomarkers that can predict the future onset of nephrotoxicity. The specific aim of the present study therefore was to develop a model for use in predicting the future onset of drug-induced renal proximal tubular injury following repeated dosing with nephrotoxics. The model was constructed based on gene expression data obtained in the single-dose studies.

In the present study, rat kidney microarray gene expression data collected following single-dose treatments with several different classes of nephrotoxic and nonnephrotoxic compounds were divided into positive and negative training sets for modeling. The data were divided based upon histopathological findings observed after up to 28 days of repeated dosing. Candidate biomarkers for predicting the future onset of proximal tubular injury were extracted using supervised classification algorithms with filter-type gene selection. For validation of the prediction model, the external test sets were randomly generated 100 times by dividing the training set into subsets, and the prediction accuracy was calculated by summarizing the prediction results of the external test sets. Although our optimized model consisted of only 19 selected probes, it achieved a sensitivity of 93% with a selectivity of 90% in predicting the future onset of tubular injury. In addition to some novel biomarker candidates, the selected genes included several well-known nephrotoxic biomarkers, such as kidney injury molecule-1 (*Kim1*) and clusterin (*Clu*). Functional annotation analysis revealed that the feature genes are involved in DNA replication, cell cycle control, apoptosis, and responses to oxidative stress and chemical stimuli. The classification accuracy of our multigene-based model was better than that of any of the well-known individual biomarkers or classical toxicological endpoints, including histopathological findings. The results of our present study suggest that toxicogenomic-based classifications

are useful in predicting the future onset of renal proximal tubular injury in rats.

2. Materials and methods

2.1. Compounds

The chemical name, abbreviation, dose, dosing route, and vehicle for each compound used in this study are summarized in Table 1.

2.2. Animal treatment

Five-week-old male Sprague-Dawley rats were obtained from Charles River Japan, Inc. (Kanagawa, Japan). After a 7-day quarantine and acclimatization period, 6-week-old animals were assigned to dosage groups (5 rats per group) using a computerized stratified random grouping method based on individual body weight. The animals were individually housed in stainless steel cages in an animal room that was illuminated for 12 h (07:00–19:00) each day, ventilated with an air-exchange rate of 15 times per hour, and maintained at 21–25 °C with a relative humidity of 40–70%. Each animal was allowed free access to water and pellet diet (CRF-1, sterilized by radiation, Oriental Yeast Co., Ltd., Tokyo, Japan). Drugs were suspended or dissolved in 0.5% methylcellulose solution (MC) or corn oil according to their dispersibility and administered to rats orally, with the exception of cisplatin, carboplatin, 2-bromoethylamine, cephalothin, puromycin aminonucleoside, gentamicin, vancomycin, and doxorubicin, which were dissolved in saline and administered intravenously. In single-dose studies, animals were euthanized 3, 6, 9, and 24 h after administration of the single dose. In repeated-dose studies, animals were treated daily for 3, 7, 14, or 28 days and euthanized 24 h after receiving the last dose. Euthanasia was carried out by exsanguination from the abdominal aorta under ether anesthesia. For histopathological examination, samples of kidney tissue were fixed in 10% neutral-buffered formalin, dehydrated in alcohol, and embedded in paraffin. Paraffin sections were prepared and stained using standard hematoxylin and eosin staining (H&E) methods. Histopathological changes were graded by a pathologist according to the following criteria: + = minimal; 2+ = slight; 3+ = moderate; and 4+ = severe. All specimens were peer-reviewed by another pathologist for confirmation of findings. The experimental protocols were reviewed and approved by the Ethics Review Committee for Animal Experimentation of the National Institute of Health Sciences.

2.3. Microarray analysis

Immediately after euthanasia, a thin slice of kidney section (transverse section; about 30 mg) was obtained from the kidney of each animal for RNA analysis. Tissue samples were kept overnight at 4 °C in RNAlater® (Ambion, Austin, TX, USA) and then frozen at –80 °C until use. Samples of kidney tissue were homogenized with the RLT buffer supplied with the RNeasy mini kit (Qiagen, Valencia, CA, USA) and total RNA was isolated according to the manufacturer's instructions. Microarray analysis was conducted on three of the five samples from each group using GeneChip® Rat Genome 230 2.0 Arrays (Affymetrix, Santa Clara, CA, USA), which contain 31,042 probes. The procedure was conducted according to the manufacturer's instructions using One-Cycle Target Labeling and Control Reagents (Affymetrix) for cDNA synthesis, purification, and the synthesis of biotin-labeled cRNA. A total of 10 µg of fragmented cRNA was hybridized to a Rat Genome 230 2.0 Array for 18 h at 45 °C at 60 rpm, after which the array was washed and stained with streptavidin–phycoerythrin using a Fluidics Station 400 (Affymetrix), and then scanned with a Gene Array Scanner (Affymetrix). The digital image files were preprocessed using Affymetrix Microarray Suite, version 5.0 (MAS5.0), and the data were converted into base10 logarithmic values. These values were normalized into Z-scores using Tukey's biweight algorithm. The normalized datasets were reversed into nonlogarithmic values by calculating their exponential numbers in decimal, and the base 2 log-ratios of the means of the control groups were calculated.

2.4. Gene selection and supervised classification

Every different combination of gene expression data collected at continuous time points (3–24 h) in the single-dose study was examined to determine the best combination of time points to use in predicting renal tubular toxicity. For machine learning and external validation purposes, the compounds were classified as either “positive” or “negative” based upon the histopathological findings (Table 2; for more detailed information, see Supplemental Table 1). The target property was proximal renal tubular injury following exposure to a given compound for up to 28 days. Briefly, a compound was designated as nephrotoxic (positive) if histopathological evidence of proximal tubular injury (e.g., tubular necrosis/degeneration, regeneration) was observed in samples from at least one time point in the repeated-dose study. According to this criterion, a high-dose group of 14 positive compounds was defined as the positive training set. The remaining nine positive compounds were excluded from the positive training set and were used as the external test set because the primary toxicity target of these compounds was the glomerulus (PAN, CPA, DOX, and HCB), juxtaglomerular apparatus (CAP and ENA), or renal papilla (LS and IM).

Table 1
Dosage and administration conditions of compounds used in the training and testing of the prediction model.

Compound	Compound (abbreviated)	Dose (mg/kg; single dose)			Dose (mg/kg/day; repeated dose)			Vehicle	Dosing route
		Low	Middle	High	Low	Middle	High		
Vancomycin hydrochloride	VMC	20	60	200	20	60	200	Saline	iv
2-Bromoethylamine hydrobromide	BEA	6	20	60	2	6	20	Saline	iv
Phenylbutazone	PhB	20	60	200	20	60	200	0.5% MC	po
Cyclosporine A	CSA	30	100	300	10	30	100	Corn oil	po
Thioacetamide	TAA	4.5	15	45	4.5	15	45	0.5% MC	po
K17	K17	60	200	600	60	200	600	0.5% MC	po
Triamterene	TRI	15	50	150	15	50	150	0.5% MC	po
Allopurinol	APL	15	50	150	15	50	150	0.5% MC	po
Nitrofurantoin	NFT	10	30	100	10	30	100	0.5% MC	po
Ethionine	ET	25	80	250	25	80	250	0.5% MC	po
N-Phenylanthranilic acid	NPAA	300	1000	2000	100	300	1000	0.5% MC	po
Cisplatin	CSP	0.3	1	3	0.1	0.3	1	Saline	iv
Phenacetin	PCT	300	1000	2000	100	300	1000	0.5% MC	po
Carboplatin	CBP	10	30	100	1	3	10	Saline	iv
Gentamicin sulphate	GMC	10	30	100	10	30	100	Saline	iv
Puromycin aminonucleoside	PAN	12	40	120	4	12	40	Saline	iv
Lomustine	LS	0.6	2	6	0.6	2	6	0.5% MC	po
Cyclophosphamide	CPA	1.5	5	15	1.5	5	15	0.5% MC	po
Hexachlorobenzene	HCB	300	1000	2000	30	100	300	Corn oil	po
Captopril	CAP	100	300	1000	100	300	1000	0.5% MC	po
Enalapril	ENA	60	200	600	60	200	600	0.5% MC	po
Indomethacin	IM	0.5	1.6	5	0.5	1.6	5	0.5% MC	po
Doxorubicin hydrochloride	DOX	1	3	10	0.1	0.3	1	Saline	iv
Ethinyl estradiol	EE	1	3	10	1	3	10	Corn oil	po
Monocrotaline	MCT	3	10	30	3	10	30	0.5% MC	po
Acetaminophen	APAP	300	600	1000	300	600	1000	0.5% MC	po
Cephalothin sodium	CLT	300	1000	2000	300	1000	2000	Saline	iv
Bucetin	BCT	300	1000	2000	100	300	1000	0.5% MC	po
Methyltestosterone	MTS	30	100	300	30	100	300	0.5% MC	po
Rifampicin	RIF	20	60	200	20	60	200	0.5% MC	po
Imipramine hydrochloride	IMI	10	30	100	10	30	100	0.5% MC	po
Acetazolamide	ACZ	60	200	600	60	200	600	0.5% MC	po
Caffeine	CAF	10	30	100	10	30	100	0.5% MC	po
Valproic acid	VPA	45	150	450	45	150	450	0.5% MC	po
Clofibrate	CFB	30	100	300	30	100	300	Corn oil	po
Allyl alcohol	AA	3	10	30	3	10	30	Corn oil	po
Omeprazole	OPZ	100	300	1000	100	300	1000	0.5% MC	po
Bromobenzene	BBZ	30	100	300	30	100	300	Corn oil	po
Ketoconazole	KC	10	30	100	10	30	100	0.5% MC	po
Ciprofloxacin	CPX	100	300	1000	100	300	1000	0.5% MC	po
Erythromycin ethylsuccinate	EME	100	300	1000	100	300	1000	0.5% MC	po

Male SD rats received oral or intravenous doses once daily (6 weeks of age, $n=5$ /group for histopathology). Kidney tissue was collected and used for gene expression analysis (Affymetrix GeneChip®, $n=3$ /group) at 3, 6, 9, and 24 h after administration in the single-dose experiment, or 4, 8, 15, and 29 days after the start of repeated dosing. po: oral administration, iv: intravenous administration, 0.5% MC: 0.5% methylcellulose solution.

Proximal injuries to these targets are believed to appear subsequent to the initial, or primary, injuries. Although GMC is thought to cause direct injury to renal tubules, no significant changes in kidney gene expression were observed in rats treated with a single dose of this compound; therefore, GMC was excluded from the training set and used in the test set. Conversely, a compound was deemed nonnephrotoxic (negative) if it did not produce adverse histopathological findings in the proximal tubule during the period of repeated dosing. Based on this criterion, eight high-dose hepatotoxic compounds which produced no histopathological findings of renal tubular injury upon chronic exposure were included in the negative set. The negative set also included a low-dose group of 31 compounds (Table 2). The additional test set included a high-dose group of 10 compounds and a middle-dose group of all the nephrotoxic and nonnephrotoxic compounds.

Supplementary material related to this article found, in the online version, at <http://dx.doi.org/10.1016/j.tox.2012.03.014>.

The training data set was used with filter-type gene selection algorithms and Support Vector Machine (SVM) supervised classification algorithms to extract biomarker candidates and construct classifiers using the selected biomarker genes. The intensity-based moderated *T*-statistic (IBMT; Sartor et al., 2006) was used as a filter-type gene selection algorithm. To estimate the performance of our classifier, a five-fold cross-validation was conducted, for which a detailed procedure was described in our previous report (Kondo et al., 2009).

2.5. Gene ontology analysis

Gene ontology (GO) analysis was conducted for feature genes selected from both the current prediction and previously developed diagnostic models, using the 99 top-ranked probes from each model. BiblioSphere PathwayEdition (Genomatix, Munich, Germany) was used for GO analysis.

3. Results

3.1. Histopathological examination

The results of histopathological examinations are summarized in Table 2. Necrosis, degeneration, and/or regeneration of the proximal tubules resulted from treatment with 23 of the proximal tubular toxicants, and chronic exposure to 6 of 10 potential tubular toxicants caused other histopathological findings. In rats receiving a single dose, only four compounds (VMC, CSA, K17, and NFT) produced histopathological signs of proximal tubular injury. These results suggest that histopathological examination alone is not sufficient for early detection of nephrotoxicity in animals treated with only a single dose. Detailed histopathological findings pertaining to all compounds at each time point and dose level are summarized in Supplemental Table 1.

3.2. Gene selection and supervised classification

We tested the prediction accuracy of the classifiers using the test set. The groups of positive and negative compounds were each randomly divided into five subsets 100 times. An arbitrary subset was used as the external test set, and the remaining subsets were used as the training set. We constructed classifiers using gene expression data from every different combination of continuous time points (3–24 h) in order to determine the most robust combination for predicting renal tubular injury. Fig. 1 shows five-fold cross-validation receiver operating characteristic (ROC) curves, each of which was generated using a different combination of continuous time points. A classifier using 24-h gene expression data alone displayed the highest prediction accuracy, and achieved a sensitivity of 93% and selectivity of 90% using 19 feature genes. In the best model, the prediction accuracy was almost saturated and was not significantly affected by increasing the number of feature genes used for modeling. The number of support vectors was adequately lowered, and the number of feature genes was substantially smaller than the number of samples to avoid over-fitting (data not shown). At around the top 19 probes, the number of support vectors gradually increased, indicating that genes ranked 20 or above provided little to no information for classification, and that adding additional genes for modeling imposes a risk of

over-fitting. We therefore concluded that the classifier constructed using the top 19 ranked probes (Table 3) was the best model. The rankings of top 99 feature genes are provided in Supplemental Table 2.

Supplementary material related to this article found, in the online version, at <http://dx.doi.org/10.1016/j.tox.2012.03.014>.

3.3. Test data set prediction performance

We also tested the prediction performance of the 24 h classifier using the test compounds. Classification results for each time point are shown in Table 2 (for detailed prediction results, see Supplemental Table 1). In the repeated-dose experiment, the sensitivity was 82% and the selectivity was 98%. All 14 of the high-dose group positive training compounds were correctly predicted as positive at one or more time points in the repeated-dose experiment, and the positive predictions primarily occurred before or at time points preceding the appearance of histopathological changes. A total of five of the middle-dose positive training compounds (BEA, CSA, TAA, K17, and NPAA) were predicted as positive at 24 h, and six of the middle-dose compounds (CSA, TAA, K17, TRI, ET, CSP, and CBP) were predicted as positive at one or more time points in the repeated-dose experiment, regardless of the presence or absence of histopathological evidence of nephrotoxicity. In addition, all of the high-dose negative training compounds were correctly predicted as negative in the repeated-dose experiment. All of the nine positive test compounds (GMC, PAN, LS, CPA, HCB, CAP, ENA, IM, and DOX) were correctly predicted as positive at the high dose in the repeated-dose experiments. Of the 10 test compounds administered at the high dose, CLT was predicted as positive in the single-dose experiment, and four compounds (EE, MCT, CLT, and APAP) were predicted as positive in the repeated-dose experiment. In contrast, two compounds (MTS and CAF) were predicted as negative in both the single- and repeated-dose experiments.

We also compared the prediction profiles generated in the present study with the diagnostic model developed in our previous work (Kondo et al., 2009) with respect to the prediction of future onset of nephrotoxicity following administration of a single dose of test compound. Low positive probabilities of toxicity were returned by the diagnostic model for TRI, NFT, ET, and PCT, while there was a negative prediction of toxicity for CLT. In contrast, the current prediction model returned positive predictions of toxicity for each of these compounds. Furthermore, BBZ, which is nonnephrotoxic, was falsely predicted as positive using our previous diagnostic model.

3.4. Gene expression profiles of the feature genes

Fig. 2 shows the gene expression profiles (24 h and day 29) of the feature genes included in the current prediction model and the previously developed diagnostic model. The *Z*-scores were calculated by dividing the log-ratio values by the variance of the log-ratio value of the control samples calculated for each arbitrary range of the expression values. The expression values for the control samples were then pooled for each compound and time point. The feature genes included in the current prediction model showed either significant upregulation or downregulation in both the single- (Fig. 2A) and repeated-dose experiments (Fig. 2B). The feature genes included in the diagnostic model exhibited relatively smaller changes in expression in the single-dose experiment (Fig. 2C) compared to the repeated-dose experiment (Fig. 2D). Many compounds produced no change in expression of the feature genes included in the diagnostic model at 24 h. Although some compounds produced pronounced up- or down-regulation in the expression of some of the feature genes included in the diagnostic model at 24 h, it was restricted to those compounds for which histopathological changes

Table 2
Summary of histopathology findings, definition of each compound for use in modeling, and prediction result for each dose and time point.

Compound	Compound abbreviation	Histopathology		Training/test	P/N label		Low					Middle					High				
		Repeated dose	Single dose		Low	High	24 h	4 days	8 days	15 days	29 days	24 h	4 days	8 days	15 days	29 days	24 h	4 days	8 days	15 days	29 days
Vancomycin hydrochloride	VMC	Yes	Yes	Training (positive)	N	P	0.01	0.01	0.01	0.00	0.02	0.04	0.01	0.01	0.01	0.04	0.91	0.91	0.84	0.92	1.00
2-Bromoethylamine hydrobromide	BEA	Yes	No	Training (positive)	–	P	0.02	0.04	0.01	0.01	0.02	1.00	0.04	0.07	0.02	0.10	1.00	0.91	0.25	0.76	0.53
Phenylbutazone	PhB	Yes	No	Training (positive)	N	P	0.01	0.11	0.03	0.12	0.04	0.01	0.05	0.05	0.07	0.15	1.00	0.87	0.27	0.76	1.00
Cyclosporine A	CSA	Yes	Yes	Training (positive)	–	P	0.07	0.03	0.01	0.03	0.06	0.78	0.01	0.68	0.41	0.80	1.00	0.54	0.96	0.92	1.00
Thioacetamide	TAA	Yes	No	Training (positive)	N	P	0.02	0.38	0.13	0.06	0.04	0.51	0.91	0.79	0.92	0.92	1.00	1.00	1.00	1.00	1.00
K17	K17	Yes	Yes	Training (positive)	N	P	0.04	0.11	0.26	0.13	0.04	0.93	0.70	0.16	0.91	0.86	1.00	1.00	1.00	1.00	1.00
Triamterene	TRI	Yes	No	Training (positive)	N	P	0.02	0.08	0.01	0.02	0.01	0.27	0.57	0.10	0.64	0.36	0.94	0.98	0.95	1.00	1.00
Allopurinol	APL	Yes	No	Training (positive)	N	P	0.02	0.04	0.01	0.07	0.08	0.13	0.06	0.16	0.04	0.08	1.00	1.00	1.00	1.00	1.00
Nitrofurantoin	NFT	Yes	Yes	Training (positive)	N	P	0.02	0.04	0.02	0.02	0.02	0.17	0.03	0.06	0.02	0.02	0.86	0.61	0.49	0.20	0.88
Ethionine	ET	Yes	No	Training (positive)	N	P	0.01	0.22	0.01	0.07	0.03	0.32	0.90	0.05	0.10	0.09	0.96	0.99	0.46	0.47	0.31
N-Phenylanthranilic acid	NPAA	Yes	No	Training (positive)	–	P	0.50	0.11	0.02	0.04	0.03	1.00	0.04	0.05	0.10	0.12	1.00	1.00	0.93	1.00	0.86
Cisplatin	CSP	Yes	No	Training (positive)	–	P	0.02	0.01	0.07	0.03	0.45	0.28	0.03	0.51	0.87	0.99	1.00	0.91	1.00	1.00	1.00
Phenacetin	PCT	Yes	No	Training (positive)	–	P	0.01	0.05	0.00	0.03	0.01	0.08	0.10	0.02	0.02	0.02	0.97	0.68	0.42	0.84	0.97
Carboplatin	CBP	Yes	No	Training (positive)	–	P	0.03	0.02	0.00	0.01	0.07	0.15	0.02	0.02	0.10	0.55	1.00	0.05	0.10	0.27	1.00
Gentamicin sulphate	GMC	Yes	No	Test	N	–	0.02	0.01	0.13	0.12	0.06	0.04	0.08	0.27	0.79	1.00	0.13	0.14	1.00	1.00	1.00
Puromycin aminonucleoside	PAN	Yes	No	Test	–	–	0.04	0.02	0.01	0.07	0.26	0.03	0.03	0.04	1.00	1.00	0.03	0.35	1.00	NA	NA
Lomustine	LS	Yes	No	Test	N	–	0.00	0.07	0.05	0.10	0.02	0.05	0.12	0.02	0.12	0.26	0.00	0.11	0.05	1.00	1.00
Cyclophosphamide	CPA	Yes	No	Test	N	–	0.05	0.06	0.04	0.02	0.01	0.03	0.05	0.03	0.02	0.02	0.05	0.07	0.12	0.13	0.85
Hexachlorobenzene	HCB	Yes	No	Test	–	–	0.08	0.02	0.02	0.04	0.25	0.01	0.04	0.05	0.06	0.89	0.02	0.03	0.14	0.37	0.92
Captopril	CAP	Yes	No	Test	N	–	0.01	0.02	0.02	0.05	0.01	0.03	0.02	0.38	0.06	0.38	0.02	0.95	0.70	0.35	0.11
Enalapril	ENA	Yes	No	Test	N	–	0.01	0.07	0.20	0.09	0.05	0.00	0.06	0.54	0.75	0.52	0.07	0.39	0.97	0.29	0.83
Indomethacin	IM	Yes	No	Test	N	–	0.04	0.10	0.01	0.03	0.01	0.03	0.09	0.02	0.11	0.03	0.07	0.42	0.38	1.00	NA
Doxorubicin hydrochloride	DOX	Yes	No	Test	–	–	0.05	0.04	0.01	0.02	0.02	0.08	0.08	0.02	0.03	0.05	0.45	0.02	0.04	0.05	1.00
Ethinyl estradiol	EE	–	–	Test	N	–	0.00	0.01	0.07	0.13	0.74	0.02	0.10	0.20	0.70	0.96	0.03	0.11	0.44	0.59	0.94
Monocrotaline	MCT	–	–	Test	N	–	0.03	0.02	0.06	0.02	0.13	0.00	0.02	0.16	0.11	0.58	0.02	0.07	0.82	1.00	NA
Acetaminophen	APAP	–	–	Test	N	–	0.03	0.04	0.11	0.05	0.04	0.03	0.16	0.11	0.07	0.34	0.05	0.18	0.06	0.66	0.78
Cephalothin sodium	CLT	–	–	Test	N	–	0.03	0.05	0.03	0.03	0.08	0.22	0.06	0.06	0.09	0.25	0.01	0.25	0.15	0.10	0.48
Bucetin	BCT	–	–	Test	–	–	0.06	0.02	0.03	0.29	0.06	0.17	0.02	0.06	0.09	0.06	0.21	0.02	0.02	0.59	0.04
Methyltestosterone	MTS	–	–	Test	N	–	0.01	0.01	0.02	0.00	0.02	0.02	0.01	0.01	0.01	0.02	0.01	0.01	0.11	0.07	0.05
Rifampicin	RIF	–	–	Test	N	–	0.06	0.06	0.02	0.05	0.00	0.02	0.02	0.07	0.06	0.13	0.10	0.42	0.14	0.09	0.41
Imipramine hydrochloride	IMI	–	–	Test	N	–	0.01	0.01	0.01	0.02	0.05	0.01	0.01	0.01	0.06	0.04	0.02	0.03	0.09	0.28	0.09
Acetazolamide	ACZ	–	–	Test	N	–	0.04	0.07	0.04	0.04	0.01	0.55	0.06	0.10	0.08	0.02	0.45	0.04	0.10	0.10	0.09
Caffeine	CAF	–	–	Test	N	–	0.03	0.02	0.05	0.05	0.02	0.04	0.01	0.03	0.02	0.06	0.05	0.02	0.01	0.07	0.02
Valproic acid	VPA	No	No	Training (negative)	N	N	0.02	0.02	0.01	0.10	0.01	0.01	0.02	0.01	0.16	0.00	0.00	0.02	0.02	0.14	0.04
Clofibrate	CFB	No	No	Training (negative)	N	N	0.03	0.03	0.10	0.05	0.06	0.06	0.03	0.03	0.03	0.06	0.09	0.09	0.10	0.17	0.13
Allyl alcohol	AA	No	No	Training (negative)	N	N	0.04	0.01	0.01	0.05	0.01	0.07	0.01	0.09	0.02	0.00	0.02	0.01	0.03	0.03	0.01
Omeprazole	OPZ	No	No	Training (negative)	N	N	0.01	0.02	0.01	0.07	0.11	0.02	0.03	0.32	0.13	0.01	0.09	0.02	0.04	0.15	0.06
Bromobenzene	BBZ	No	No	Training (negative)	N	N	0.01	0.02	0.01	0.06	0.01	0.01	0.06	0.01	0.10	0.01	0.08	0.03	0.02	0.05	0.06
Ketoconazole	KC	No	No	Training (negative)	N	N	0.01	0.01	0.04	0.02	0.01	0.03	0.03	0.04	0.01	0.01	0.05	0.02	0.08	0.02	0.03
Ciprofloxacin	CPX	No	No	Training (negative)	N	N	0.05	0.04	0.06	0.04	0.02	0.06	0.02	0.04	0.04	0.01	0.02	0.01	0.02	0.06	0.03
Erythromycin ethylsuccinate	EME	No	No	Training (negative)	N	N	0.00	0.02	0.04	0.03	0.08	0.02	0.02	0.03	0.01	0.06	0.04	0.07	0.12	0.05	0.07

Definition of the training set (P: positive, N: negative). The absence or presence of proximal tubular toxicity is indicated by No or Yes, respectively, based upon the absence or presence of the following histopathological findings: necrosis, degeneration, regeneration. Positive predictions are highlighted in gray.

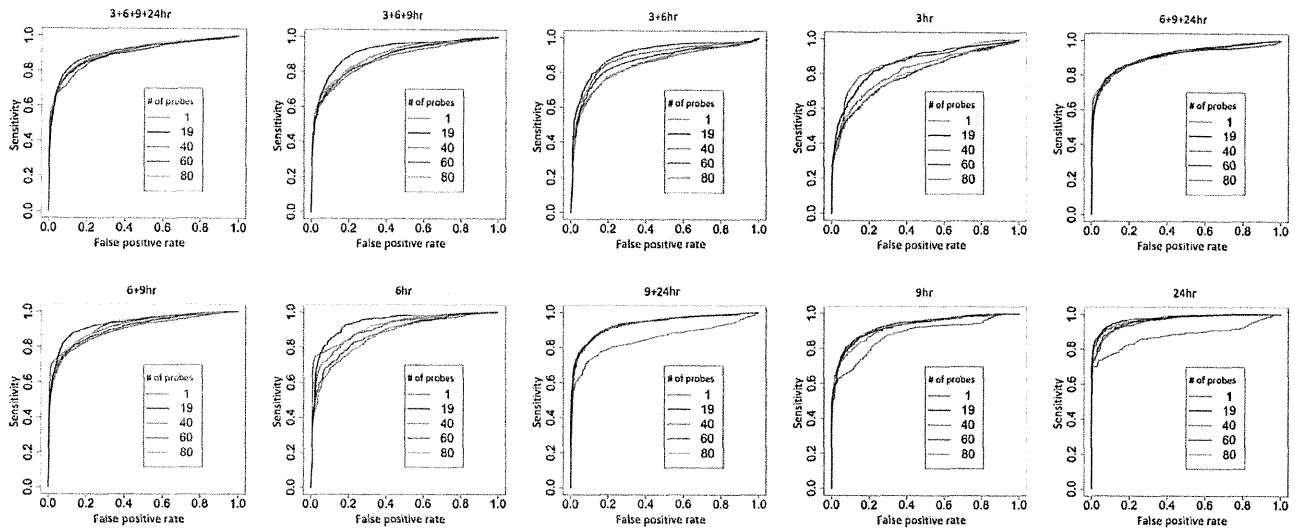


Fig. 1. ROC curve of the models using gene expression data from every different combination of continuous time points (3–24 h).

were also observed at 24 h. In addition, the extent of the changes in expression observed for the genes included in the diagnostic model was comparatively smaller than the extent of the changes observed in the genes included in the current prediction model. Regarding the ranking of feature genes using the IBMT statistic, the feature genes included in the prediction model were ranked relatively low in the list of genes included in the diagnostic model.

3.5. Gene ontology analysis

GO analysis was conducted for feature genes selected from both the current prediction and previously developed diagnostic models. The prediction model was enriched with genes involved in DNA replication, cell cycle control, apoptosis, oxidative stress responses, and responses to chemical stimuli (Supplemental Table 3A), while the diagnostic model was enriched with genes involved in tissue remodeling, inflammatory responses, cell growth, blood coagulation, and homeostasis (Supplemental Table 3B).

Supplementary material related to this article found, in the online version, at <http://dx.doi.org/10.1016/j.tox.2012.03.014>.

4. Discussion

In this research, we constructed a novel model for predicting renal proximal tubular injury in rats. The prediction model was developed based upon gene expression profiles determined following administration of single doses of different classes of nephrotoxic and nonnephrotoxic compounds. Models were constructed using all possible combinations of data collected at each continuous time point (3, 6, 9, and 24 h) to determine the combination of gene expression changes that is most effective in predicting proximal tubular injury. The prediction accuracy gradually increased with time after dosing in constructing the model. We identified a number of genes that are differentially expressed at 24 h post-administration and which predict proximal tubular injury with a high degree of accuracy and sensitivity. Our results suggested that gene expression changes that occur soon after administration predominantly reflect chemical class-specific mechanisms of toxicity rather than the likelihood of renal tubular injury, and are thus not suitable for use in models aimed at predicting the future onset of injury induced by different classes of toxicants. We therefore concluded that 24 h after administration of a single dose of

Table 3
List of the 19 feature genes included in the prediction model.

Probe ID	Rank	IBMT value	Gene title	Gene symbol
1387965_at	1	13.1	Hepatitis A virus cellular receptor 1	<i>Havcr1</i>
1368420_at	2	11.1	Ceruloplasmin	<i>Cp</i>
1368627_at	3	-10.9	Regucalcin (senescence marker protein-30)	<i>Rgn</i>
1368497_at	4	10.8	ATP-binding cassette, sub-family C (CFTR/MRP), member 2	<i>Abcc2</i>
1370445_at	5	10.7	Phospholipase A1 member A	<i>Pla1a</i>
1371785_at	6	10.4	Tumor necrosis factor receptor superfamily, member 12a	<i>Tnfrsf12a</i>
1383605_at	7	-10.3	Similar to alpha-fetoprotein	<i>LOC360919/LOC684913</i>
1379889_at	8	10.1	Laminin, gamma 2	<i>Lamc2</i>
1377092_at	9	9.5	EST	<i>EST</i>
1379340_at	10	9.5	Laminin, gamma 2	<i>Lamc2</i>
1390579_at	11	9.4	Similar to RIKEN cDNA 1810029B16	<i>RGD1305222</i>
1387382_at	12	-9.3	Histamine N-methyltransferase	<i>Hnmt</i>
1370422_at	13	9.2	Receptor-interacting serine-threonine kinase 3	<i>Ripk3</i>
1367856_at	14	9.1	Glucose-6-phosphate dehydrogenase	<i>G6pd</i>
1370333_a.at	15	-9.0	Insulin-like growth factor 1	<i>Igf1</i>
1367712_at	16	9.0	TIMP metalloproteinase inhibitor 1	<i>Timp1</i>
1367977_at	17	-8.9	Synuclein, alpha (non A4 component of amyloid precursor)	<i>Snca</i>
1374070_at	18	8.8	Glutathione peroxidase 2	<i>Gpx2</i>
1383675_at	19	8.6	EST	<i>EST</i>

Genes were ranked using the intensity-based modified T-statistic.

nephrotoxic compound was the best time point for use in modeling because the gene expression changes indicative of renal tubular injury observed at that time point were similar in rats treated with different classes of compounds. Changes in the expression of the feature genes occurring 24 h after administration probably reflect secondary downstream signals rather than a primary response to injuries induced by specific individual compounds. Although we only focused on gene expression changes that are common to exposure to several different classes of nephrotoxics, the gene expression profiles observed at earlier time points, such as 3, 6, and 9 h after administration, were heterogeneous. Further detailed analyses focusing on the gene expression profile associated with exposure to each class of compound might provide useful information regarding the mechanism through which these compounds cause tubular injury and may lead to the discovery of mechanism-specific gene-based biomarkers.

In constructing the prediction model, we employed typical nephrotoxic compounds that directly cause proximal renal tubular injury as well as several compounds that have diverse nephrotoxic effects and different patterns of histopathological changes, and examined their impact on gene expression at multiple-time points and dosages. In rats subjected to repeated doses for up to 28 days, 23 compounds produced proximal tubular injury and were thus classified as “positive”. Of these positive compounds, only 14 were used for modeling. The remaining compounds were excluded because they primarily targeted other parts of the nephron or exhibited nephrotoxicity only at the latter time point (i.e., day 29) in the repeated-dose study. Before modeling, we constructed a classifier that included all 23 nephrotoxic compounds in the positive set; however, the prediction accuracy obtained with this classifier was poor (data not shown). In contrast, a high degree of prediction accuracy was obtained in our best model trained with the smaller 14-compound data set. For example, our model correctly predicted renal tubular injury following repeated administration of these 14 nephrotoxic compounds. Of positive compounds, CBP, which directly injure the proximal renal tubule but which produced no observable histopathological signs of renal tubular injury until day 29 following repeated dosing, was correctly predicted as “positive”. In addition, the model returned a positive prediction in the repeated-dose experiment for the remaining positive compounds, which were excluded from modeling, although the model did not return a positive prediction in the single-dose experiment. We therefore concluded that these 14 nephrotoxic compounds was the best choice for feature gene selection and remaining 9 compounds were not sufficient for use in modeling because the gene expression changes indicative of renal tubular injury observed at that time point were not observed. Furthermore, primary toxicological changes, such as glomerular or papillary injury, are considered to be needed prior to the onset of proximal tubular injury when these compounds are repeatedly administered. Although our current model successfully predicted future onset of proximal tubular injury induced by various different classes of nephrotoxics using feature genes occurring 24 h after administration, no positive predictions were observed in these remaining 9 compounds. This will be a potential limitation of our prediction model, since for most compounds, steady state levels have likely not been reached at that time point in the single dose study.

In the present study, we tested the prediction performance of the 24 h classifier using the test compounds. Of the positive training compounds, all of the high-dose groups were correctly predicted as positive at one or more time points in the repeated-dose experiment. In contrast, of the 10 negative test compounds administered at the high dose, CLT was predicted as positive in the single-dose experiment, and four compounds (EE, MCT, CLT, and APAP) were predicted as positive in the repeated-dose experiment. Although these test compounds produced no direct evidence of

nephrotoxicity under our experimental conditions, vacuolar changes and dilatation in the proximal tubule (EE) as well as single cell necrosis and anisonucleosis in the mesangial cells (MCT) were observed in animals subjected to repeated-doses. Thus, positive predictions for EE and MCT were considered to reflect these histopathological findings. Although no histopathological findings were observed under our experimental conditions in rats administered CLT and APAP, these compounds are potential nephrotoxics. For example, APAP is known to induce nephrotoxicity in rats (Das et al., 2010). Renal insufficiency reportedly occurs in approximately 1–2% of acetaminophen overdose patients (Mazer and Perrone, 2008). Although CLT is a second-generation cephalosporin antibiotic with a reduced potential for nephrotoxicity, the cephalosporin antibiotics may commonly produce toxicity in the kidneys (Zhan, 1990). It is therefore reasonable to conclude that the positive predictions for CLT and APAP in the present study reflect early slight nephrotoxicity induced by treatment with these compounds.

In our previous research (Kondo et al., 2009) we used microarray data derived from repeated-dose studies to construct a diagnostic model for predicting the onset of renal tubular injury. To characterize the differences between that model and the present prediction model, we compared the expression profiles of the feature genes included in each model. Expression of the feature genes included in the present prediction model was clearly altered upon either single- or repeated-administration (Fig. 2). In contrast, expression of the feature genes included in our previously reported diagnostic model was altered 24 h following administration only in rats dosed with nephrotoxic compounds that cause renal tubular injury within 24 h. Little or no change was observed in the expression of these feature genes included in the previously described diagnostic model in rats administered nephrotoxic compounds that do not cause histopathological signs of renal tubular injury within 24 h.

The genes included in the present prediction model are primarily involved in DNA replication, cell cycle control, apoptosis, oxidative stress responses, and responses to chemical stimuli, in contrast to the genes included in the previously described diagnostic model, which are primarily involved in tissue remodeling, inflammatory responses, cell growth, blood coagulation, and homeostasis. These differences in gene function suggest that changes in the expression of the genes included in the present prediction model are indicative of the renal response to the toxic effects of the compounds that occur before histopathological changes can be observed, while changes in the expression of those genes included in the diagnostic model reflect tissue repair processes and/or disturbed homeostasis in the renal tubules. Gene expression data obtained from the single-dose experiment was used to optimize the present model for early prediction of the onset of renal tubular injury, while our previously described diagnostic model was optimized for diagnostic purposes using gene expression data generated in the repeated-dose experiment. The choice of which model to use thus depends upon research objectives.

Several recent reports described new biomarkers for predicting and monitoring early or acute nephrotoxicity. The Predictive Safety Testing Consortium's (PSTC) Nephrotoxicity Working Group recently published a report concerning the qualification of seven urinary biomarkers of nephrotoxicity (total protein, albumin, KIM-1, clusterin, β_2 -microglobulin, cystatin C, and trefoil factor 3) for limited use in nonclinical and clinical drug development to help guide safety assessments (Dieterle et al., 2010). Both *Kim1* and *Clu* (which encode KIM-1 and clusterin, respectively) were included as feature genes in the prediction model described here. Our results suggest that expression of *Kim1* and *Clu* is commonly induced by the diverse classes of nephrotoxic compounds we examined. Both KIM-1 and clusterin are excreted into the urine, and thus could be used as biomarkers for noninvasive monitoring of kidney injury.

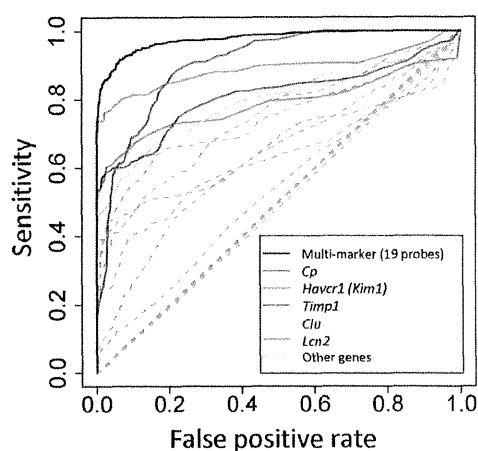


Fig. 3. ROC curve of the multigene-based toxicogenomic model in the present study and the well-known genomic biomarkers in the previous report. The classification accuracy of our multigene-based model is better than that of any of the well-known individual biomarkers.

Wang et al. (2008) evaluated a panel of 48 genes selected through a literature survey for their potential usefulness as genomic biomarkers of nephrotoxicity. The authors identified 24 genes that were differentially expressed in the kidneys of rats treated with various nephrotoxicants. The training data were used to compare the prediction performance of these individual genomic biomarkers and the toxicogenomic prediction model described in this work. The comparison study indicated that the prediction accuracy of our toxicogenomic model was much better than that obtained from any of the well-known genomic biomarkers in the previous report (Fig. 3). Our results thus suggest that the toxicogenomics-based nephrotoxicity prediction model we developed would be a useful decision making tool in the early stages of preclinical drug development. However, since our database lacks any urinary biomarker data, we could not evaluate the prediction performance of our toxicogenomic approach in comparison with proteomic or metabolomic biomarkers. A systems toxicology approach will be required for comparison and combination of biomarkers obtained by these different approaches.

In conclusion, we developed a novel toxicogenomic model that predicts the future onset of proximal tubular injury with improved accuracy. We used a large-scale and well-designed toxicogenomics database, TG-GATES, for modeling and successfully identified robust feature genes, which are commonly induced in the kidneys of rats following administration of a wide variety of nephrotoxicants. Lack of predictive reproducibility of models constructed by using relatively small scale dataset and applying inadequate modeling strategies is one of the major issues in the field of toxicogenomic research. We therefore should consider the importance of robust database curation to obtain valuable predictive tools. We also found that compounds that produce different patterns of histopathological change (e.g., time of onset, severity, type of histopathological findings) induce a heterogeneous pattern of gene expression, for which the underlying mechanisms remain to be elucidated. Although further large-scale studies will be needed before the genes included in the model could be used as robust biomarkers of nephrotoxicity, our results indicate that predictions generated by our toxicogenomic model would be valuable in screening drug candidates for potential nephrotoxicity. To facilitate use of the model in toxicological decision making, particularly in a regulatory decision making, further validation studies involving large-scale datasets evaluated using several different experimental platforms will be necessary. Such studies will ultimately lead to the

development of a gold-standard strategy for early and convenient prediction of nephrotoxicity.

Conflict of interest statement

None.

Acknowledgement

This work was supported in part by grants from the Ministry of Health, Labour and Welfare of Japan, H14-001-Toxico and H19-001-Toxico.

References

- Amin, R.P., Vickers, A.E., Sistare, F., Thompson, K.L., Roman, R.J., Lawton, M., Kramer, J., Hamadeh, H.K., Collins, J., Grissom, S., Bennett, L., Tucker, C.J., Wild, S., Kind, C., Oreffo, V., Davis 2nd, J.W., Curtiss, S., Naciff, J.M., Cunningham, M., Tennant, R., Stevens, J., Car, B., Bertram, T.A., Afshari, C.A., 2004. Identification of putative gene based markers of renal toxicity. *Environ. Health Perspect.* 112, 465–479.
- Das, J., Ghosh, J., Manna, P., Sil, P.C., 2010. Taurine protects acetaminophen-induced oxidative damage in mice kidney through APAP urinary excretion and CYP2E1 inactivation. *Toxicology* 269, 24–34.
- Dieterle, F., Sistare, F., Goodsaid, F., Papaluca, M., Ozer, J.S., Webb, C.P., Baer, W., Senagore, A., Schipper, M.J., Vonderscher, J., Sultana, S., Gerhold, D.L., Phillips, J.A., Maurer, G., Carl, K., Laurie, D., Harpur, E., Sonee, M., Ennulat, D., Holder, D., Andrews-Cleavenger, D., Gu, Y.Z., Thompson, K.L., Goering, P.L., Vidal, J.M., Abadie, E., Maciulaitis, R., Jacobson-Kram, D., Defelice, A.F., Hausner, E.A., Blank, M., Thompson, A., Harlow, P., Throckmorton, D., Xiao, S., Xu, N., Taylor, W., Vamvakas, S., Flamion, B., Lima, B.S., Kasper, P., Pasanen, M., Prasad, K., Troth, S., Bounous, D., Robinson-Gravatt, D., Betton, G., Davis, M.A., Akunda, J., McDuffie, J.E., Suter, L., Obert, L., Guffroy, M., Pinches, M., Jayadev, S., Blomme, E.A., Beushausen, S.A., Barlow, V.G., Collins, N., Waring, J., Honor, D., Snook, S., Lee, J., Rossi, P., Walker, E., Mattes, W., 2010. Renal biomarker qualification submission: a dialog between the FDA-EMEA and Predictive Safety Testing Consortium. *Nat. Biotechnol.* 28, 455–462.
- Fielden, M.R., Eynon, B.P., Natsoulis, G., Jarnagin, K., Banas, D., Kolaja, K.L., 2005. A gene expression signature that predicts the future onset of drug-induced renal tubular toxicity. *Toxicol. Pathol.* 33, 675–683.
- Gao, W., Mizukawa, Y., Nakatsu, N., Minowa, Y., Yamada, H., Ohno, Y., Urushidani, T., 2010. Mechanism-based biomarker gene sets for glutathione depletion-related hepatotoxicity in rats. *Toxicol. Appl. Pharmacol.* 247, 211–221.
- Goodsaid, F.M., Blank, M., Dieterle, F., Harlow, P., Hausner, E., Sistare, F., Thompson, A., Vonderscher, J., 2009. Novel biomarkers of acute kidney toxicity. *Clin. Pharmacol. Ther.* 86, 490–496.
- Hirode, M., Ono, A., Miyagishima, T., Nagao, T., Ohno, Y., Urushidani, T., 2008. Gene expression profiling in rat liver treated with compounds inducing phospholipidosis. *Toxicol. Appl. Pharmacol.* 229, 290–299.
- Hirode, M., Omura, K., Kiyosawa, N., Uehara, T., Shimuzu, T., Ono, A., Miyagishima, T., Nagao, T., Ohno, Y., Urushidani, T., 2009. Gene expression profiling in rat liver treated with various hepatotoxic-compounds inducing coagulopathy. *J. Toxicol. Sci.* 34, 281–293.
- Huang, Q., 2nd, Dunn R.D., Jayadev, S., DiSorbo, O., Pack, F.D., Farr, S.B., Stoll, R.E., Blanchard, K.T., 2001. Assessment of cisplatin-induced nephrotoxicity by microarray technology. *Toxicol. Sci.* 63, 196–207.
- Jiang, Y., Gerhold, D.L., Holder, D.J., Figueroa, D.J., Bailey, W.J., Guan, P., Skopek, T.R., Sistare, F.D., Sina, J.F., 2007. Diagnosis of drug-induced renal tubular toxicity using global gene expression profiles. *J. Transl. Med.* 5, 47.
- Kondo, C., Minowa, Y., Uehara, T., Okuno, Y., Nakatsu, N., Ono, A., Maruyama, T., Kato, I., Yamate, J., Yamada, H., Ohno, Y., Urushidani, T., 2009. Identification of genomic biomarkers for concurrent diagnosis of drug-induced renal tubular injury using a large-scale toxicogenomics database. *Toxicology* 265, 15–26.
- Mazer, M., Perrone, J., 2008. Acetaminophen-induced nephrotoxicity: pathophysiology, clinical manifestations, and management. *J. Med. Toxicol.* 4, 2–6.
- Ransohoff, D.F., 2004. Rules of evidence for cancer molecular-marker discovery and validation. *Nat. Rev. Cancer* 4, 309–314.
- Sartor, M.A., Tomlinson, C.R., Wesselkamper, S.C., Sivaganesan, S., Leikauf, G.D., Medvedovic, M., 2006. Intensity-based hierarchical Bayes method improves testing for differentially expressed genes in microarray experiments. *BMC Bioinformatics* 7, 538.
- Somorjai, R.L., Dolenko, B., Baumgartner, R., 2003. Class prediction and discovery using gene microarray and proteomics mass spectroscopy data: curses, caveats, cautions. *Bioinformatics* 19, 1484–1491.
- Thukral, S.K., Nordone, P.J., Hu, R., Sullivan, L., Galambos, E., Fitzpatrick, V.D., Healy, L., Bass, M.B., Cosenza, M.E., Afshari, C.A., 2005. Prediction of nephrotoxicant action and identification of candidate toxicity-related biomarkers. *Toxicol. Pathol.* 33, 343–355.

- Uehara, T., Ono, A., Maruyama, T., Kato, I., Yamada, H., Ohno, Y., Urushidani, T., 2010. The Japanese toxicogenomics project: application of toxicogenomics. *Mol. Nutr. Food Res.* 54, 218–227.
- Uehara, T., Hirode, M., Ono, A., Kiyosawa, N., Omura, K., Shimizu, T., Mizukawa, Y., Miyagishima, T., Nagao, T., Urushidani, T., 2008. A toxicogenomics approach for early assessment of potential non-genotoxic hepatocarcinogenicity of chemicals in rats. *Toxicology* 250, 15–26.
- Uehara, T., Minowa, Y., Morikawa, Y., Kondo, C., Maruyama, T., Kato, I., Nakatsu, N., Igarashi, Y., Ono, A., Hayashi, H., Mitsumori, K., Yamada, H., Ohno, Y., Urushidani, T., 2011. Prediction model of potential hepatocarcinogenicity of rat hepatocarcinogens using a large-scale toxicogenomics database. *Toxicol. Appl. Pharmacol.* 255, 297–306.
- Urushidani, T., 2010. Toxicogenomics Project and drug safety evaluation. *Nihon Yakurigaku Zasshi* 136, 46–49.
- Urushidani, T., Nagao, T., 2005. Toxicogenomics: the Japanese initiative. In: Borlak, J. (Ed.), *Handbook of Toxicogenomics-Strategies and Applications*. Wiley-VCH, Weinheim, pp. 623–631.
- Wang, E.J., Snyder, R.D., Fielden, M.R., Smith, R.J., Gu, Y.Z., 2008. Validation of putative genomic biomarkers of nephrotoxicity in rats. *Toxicology* 246 (2–3), 91–100 [Epub 2008 Jan 16].
- Zhanel, G.G., 1990. Cephalosporin-induced nephrotoxicity: does it exist? *DICP* 24, 262–265.



RNAi suppression of rice endogenous storage proteins enhances the production of rice-based *Botulinum* neurotoxin type A vaccine

Yoshikazu Yuki^{a,*}, Mio Mejima^a, Shiho Kurokawa^a, Tomoko Hiroiwa^a, Il Gyu Kong^a, Masaharu Kuroda^b, Yoko Takahashi^a, Tomonori Nochi^a, Daisuke Tokuhara^a, Tomoko Kohda^c, Shunji Kozaki^c, Hiroshi Kiyono^a

^a Division of Mucosal Immunology, Department of Microbiology and Immunology, The Institute of Medical Science, The University of Tokyo, Tokyo, 108-8639, Japan

^b Rice Physiology Research Team, National Agriculture Research Center, Niigata, Japan

^c Laboratory of Veterinary Epidemiology, Department of Veterinary Science, Graduate School of Life and Environmental Sciences, Osaka Prefecture University, Osaka, Japan

ARTICLE INFO

Article history:

Received 1 March 2012

Received in revised form 14 April 2012

Accepted 18 April 2012

Available online 1 May 2012

Keywords:

Rice

Nasal vaccine

MucoRice

RNAi

Botulinum neurotoxin

ABSTRACT

Mucosal vaccines based on rice (MucoRice) offer a highly practical and cost-effective strategy for vaccinating large populations against mucosal infections. However, the limitation of low expression and yield of vaccine antigens with high molecular weight remains to be overcome. Here, we introduced RNAi technology to advance the MucoRice system by co-introducing antisense sequences specific for genes encoding endogenous rice storage proteins to minimize storage protein production and allow more space for the accumulation of vaccine antigen in rice seed. When we used RNAi suppression of a combination of major rice endogenous storage proteins, 13 kDa prolamin and glutelin A in a T-DNA vector, we could highly express a vaccine comprising the 45 kDa C-terminal half of the heavy chain of botulinum type A neurotoxin (BoHc), at an average of 100 µg per seed (MucoRice-BoHc). The MucoRice-Hc was water soluble, and was expressed in the cytoplasm but not in protein body I or II of rice seeds. Thus, our adaptation of the RNAi system improved the yield of a vaccine antigen with a high molecular weight. When the mucosal immunogenicity of the purified MucoRice-BoHc was examined, the vaccine induced protective immunity against a challenge with botulinum type A neurotoxin in mice. These findings demonstrate the efficiency and utility of the advanced MucoRice system as an innovative vaccine production system for generating highly immunogenic mucosal vaccines of high-molecular-weight antigens.

© 2012 Elsevier Ltd. All rights reserved.

1. Introduction

Although several plants have been shown to be useful for vaccine production [1], there is accumulating evidence that the seed crop rice is one of the most suitable systems for vaccine production, storage, and delivery [2]. We have previously developed rice expressing the B subunit of cholera toxin (CTB) vaccine, MucoRice-CTB, which possesses mucosal immunogenicity and prevents diarrhea in the event of *V. cholerae* and heat-labile enterotoxin-producing enterotoxigenic *Escherichia coli* challenges

[3–6]. This rice-based vaccine has proven to be stable at room temperature for three years and thus could be used as a cold-chain-free vaccine [3,6].

In this study, we co-introduced antisense sequences specific for genes encoding endogenous rice storage proteins to block expression of these proteins and allow space for the increased accumulation of vaccine antigen in rice seed [7]. A previous report showed the feasibility of increasing the accumulation of an endogenous seed storage protein, cruciferin, by using an antisense sequence to reduce the production of another authentic seed protein (napin) in *Brassica napus* seeds [8]. In general, there are two types of protein storage organelles, called protein bodies (PB-I and -II), in rice seeds. Alcohol-soluble prolamins are expressed in PB-I (10, 13, 16 kDa) and alkali-soluble glutelins (A and B) are expressed in PB-II [9–11]. To examine whether suppression of the production of prolamins or glutelins can effectively increase the expression of a transgene-encoded vaccine antigen, we investigated the effects of RNAi suppression of 13 kDa prolamin and/or glutelin A in a T-DNA vector on expression of a candidate vaccine.

To increase the versatility of the MucoRice system, it is necessary to develop high-yield vaccines for antigens with high molecular

Abbreviations: Ab, antibody; BoHc, a nontoxic subunit fragment of *Clostridium botulinum* type-A neurotoxin; BoNT/A, *C. botulinum* neurotoxin type-A; CT, cholera toxin; CTB, cholera toxin B-subunit; ELISA, Enzyme-linked immunosorbent assay; ER, endoplasmic reticulum; LPS, lipopolysaccharide; mCTA/LTB, A subunit of mutant cholera toxin E112K with the pentameric B subunit of heat-labile enterotoxin from enterotoxigenic *Escherichia coli*; PB, protein body; PBS, phosphate-buffered saline; RNAi, RNA interference; SDS-PAGE, SDS-polyacrylamide gel electrophoresis; SigA, secretory IgA; T-DNA, transfer DNA.

* Corresponding author. Tel.: +81 3 5449 5274; fax: +81 3 5449 5411.

E-mail address: yukiy@ims.u-tokyo.ac.jp (Y. Yuki).

weight. In the original study, we successfully expressed a low-molecular-weight CTB antigen (monomer, 11 kDa) at 30 µg per seed [3]. Here, we chose a nontoxic 45 kDa fragment of the C-terminal half of the heavy chain of botulinum neurotoxin type A (BoHc) to use as an example of a high-molecular-weight vaccine antigen to evaluate the advanced MucoRice expression system. Although the botulinum neurotoxin is known as oral poisons and is absorbed from the gut to reach peripheral nerve terminals via the blood circulation, the toxin also acts as an inhalant poison, which is absorbed from the airway [12]. The Hc fragment of type A (BoHc) has been successfully used as a nasal vaccine against botulism in mice and nonhuman primates [13].

Here, we could successfully express high yields of high molecular-weight BoHc in a soluble form with the use of an optimized RNAi vector. Because the rice-based BoHc vaccine (or MucoRice-BoHc) was water-soluble and could be purified easily by standard gel filtration, our results demonstrate that advanced MucoRice system can be used for the preparation of purified antigen for nasal immunization and the induction of protective immunity against a neurological toxin.

2. Materials and methods

2.1. DNA construction, transformation of rice plants, and purification of rice-based BoHc

The sequences encoding BoHc were synthesized with optimized codon usage for rice [3] and inserted into a binary T-DNA vector (pZH2B/35SNos) [14] with an overexpressing cassette of BoHc and a combination cassette for RNAi suppression of either 13 kDa prolamin or glutelin A or both storage proteins (Fig. 1A) as described previously [7]. A RNAi cassette containing no RNAi trigger sequences for rice endogenous storage proteins was called pZH2BiK. RNAi cassettes containing RNAi trigger sequences for the suppression of the genes encoding 13 kDa prolamin and glutelin A were constructed and called pZH2Bik45 and pZH2BikG1B, respectively. The RNAi trigger sequence for the gene encoding 13 kDa prolamin was a 45 bp fragment of rice 13 kDa prolamin gene comprising coding sequence 1–45. The RNAi trigger sequence for glutelin gene was a 129 bp fragment of the rice glutelin A gene comprising coding sequence 142–270. The *Acs 1–Mul 1* fragment of the BoHc expression cassette was subcloned into pZH2BiK, pZH2Bik45, pZH2BikG1B, and pZH2Bik45-G1B. The expression vectors were used to transform a japonica variety of rice, *Nipponbare*, by using an *Agrobacterium*-mediated method described previously [3] and the recombinant BoHc produced was termed MucoRice-BoHc. The rice expressing BoHc together with a combination cassette for RNAi suppression of both 13 kDa prolamin and glutelin A was polished and extracted by using PBS and then purified by using gel filtration on a Sephadex G-100 column.

2.2. Preparation of recombinant proteins

A recombinant BoHc was constructed and produced by use of the *E. coli* expression system as previously described [13]. A nontoxic form of chimeric mucosal adjuvant that combines the A subunit of mutant cholera toxin E112K with the pentameric B subunit of heat-labile enterotoxin from enterotoxigenic *E. coli* (mCTA/LTB) was constructed and produced by use of the *Brevibacillus choshinensis* expression system as previously described [15]. The level of LPS contamination in the purified BoHc and mCTA/LTB (<10 endotoxin units/mg protein) were measured by using a Limulus Test (Wako).

2.3. Protein analyses

Total seed protein was extracted from transgenic rice plant seeds as described previously [3]. Briefly, seeds of rice plants were ground to a fine powder by using a Multibeads shocker (Yasui Kikai, Osaka, Japan) and extracted in the sample buffer (2% [w/v] SDS, 5% [w/v] β-mercaptoethanol, 50 mM Tris-HCl [pH 6.8], and 20% [w/v] glycerol) and the proteins were separated by SDS-PAGE followed by Western blot analysis with rabbit anti-BoHc antibody (Ab), which was established in our laboratory using *E. coli*-derived recombinant BoHc. The level of BoHc accumulated in the rice seeds was determined by densitometry analysis of a Western blot against a standard curve generated with the use of purified *E. coli*-derived BoHc, as previously described [3].

2.4. Immunohistochemical and immune electronmicroscopic analyses

To microscopically evaluate the localization of BoHc in the MucoRice-BoHc seed, a frozen section of the rice seed was reacted with polyclonal rabbit anti-BoHc Ab and visualized with the use of 3,3'-diaminobenzidine. We confirmed that normal rabbit IgG as a control showed no immune-reactivity in MucoRice-BoHc seed. The distribution of BoHc expressed in rice seeds was analyzed by using immunoelectron microscopy with polyclonal rabbit anti-BoHc Ab as described previously [16].

2.5. Immunization, sample preparation and ELISA for detection of BoHc-Ab

To examine the mucosal immunogenicity of MucoRice-BoHc, the purified material of MucoRice-BoHc (100 µg) alone, *E. coli*-derived rBoHc (100 µg) alone, MucoRice-BoHc (25 µg) with or without CT (1 µg, List Biological Laboratories, Campbell, CA) or MucoRice-BoHc (25 µg) with mCTA/LTB (10 µg) dissolved in 20 µl of PBS, or PBS vehicle alone was intranasally immunized in mice (10 µl/nostril, *N* = 10) on 3 occasions at 1 wk intervals. The serum and nasal wash were collected prior to immunization, and 1 wk after each immunization. BoHc-specific Ab responses were determined by using BoHc-specific enzyme-linked immunosorbent assay (ELISA) as described previously [17]. Endpoint titers were expressed as the reciprocal log₂ of the last dilution that gave an OD₄₅₀ of 0.1 greater than that of the negative control.

2.6. Preparation of botulinum neurotoxin A (BoNT/A)

BoNT/A from *C. botulinum* type-A 62 was purified from the culture supernatant as previously described [18]. The toxicity of purified BoNT/A (1.1 × 10⁸ mouse i.p. LD₅₀/mg protein) was assayed by time to death after intravenous injection into mice [19].

2.7. Neutralizing assay

To analyze the protective activity of antigen-specific mucosal Ab immune responses induced by the use of purified MucoRice-BoHc as a nasal vaccine against toxin-induced neurological death, we performed a toxin challenge study, as described previously with some modification [17]. Briefly, the immunized mice were intraperitoneally challenged with 100 ng (1.1 × 10⁴ i.p. LD₅₀) or 500 ng of BoNT/A (5.5 × 10⁴ i.p. LD₅₀) diluted in 100 µl of 0.2% gelatin/PBS, and their survival was observed for 7 days.